REPORT DOCUMENTATION PAGE

Form Approved
OMB NO. 0704-0188

1. AGENCY USE ONLY (Leave Blank)	2. REPORT DATE November 14, 2001	3. REPORT TYPE AND DATES COVERED Final 15 Feb 98 - 14 Aug 01

4. TITLE AND SUBTITLE

High Strength Steel Weldment Reliability

5. FUNDING NUMBERS

DAAG55-98-1-0085

6. AUTHOR(S)

D.L. Olson

7. PERFORMING ORGANIZATION NAME(S) AND ADDRESS(ES)

Colorado School of Mines
Dept. of Met. and Mat. Eng.
Center for Welding, Joining and Coating Research
Golden, Colorado 80401-1887

8. PERFORMING ORGANIZATION REPORT NUMBER

CSM-MT-CWJCR-001-022

9. SPONSORING / MONITORING AGENCY NAME(S) AND ADDRESS(ES)

U. S. Army Research Office
P.O. Box 12211
Research Triangle Park, NC 27709-2211

10. SPONSORING / MONITORING AGENCY REPORT NUMBER

p-37378-MS .22

11. SUPPLEMENTARY NOTES

The views, opinions and/or findings contained in this report are those of the author(s) and should not be construed as an official Department of the Army position, policy or decision, unless so designated by other documentation.

12 a. DISTRIBUTION / AVAILABILITY STATEMENT

Approved for public release; distribution unlimited.

12 b. DISTRIBUTION CODE

13. ABSTRACT (Maximum 200 words)

The development of methods to control the diffusible hydrogen content during high strength steel welding was performed. The perfection of the use of irreversible weld metal hydrogen traps was demonstrated. Efforts have effectively alleviated the available diffusible hydrogen, and thus the susceptibility of hydrogen assisted cracking, by the use of ferro-yttrium additions to the welding consumable. The range of welding parameter for the most effective use of yttrium as a hydrogen getter was determined.

The investigation of the influence of retained austenite on cracking susceptibility was also investigated. Issues regarding the amount of acceptable retained austenite and its tendency to release hydrogen upon changes of service temperature and stress were evaluated.

The development of an advanced measuring apparatus for diffusible hydrogen content based on electronic, optical, and magnetic property measurements was investigated. The effort is searching for a rapid and accurate determination for both diffusible hydrogen content and distribution. This investigation used the instrumentation acquired during the DURIP grant program. Optoelectronic property measurements of color shifts in WO_3, which was attached to the steel in the form of a thin film detector, have successfully measured the diffusible hydrogen content of higher strength steel hydrogen contents. Preliminary results have also illustrated that both magnetic property and thermo electric (Seebeck) coefficient measurements can also be used to assess hydrogen issues in steel. The Seebeck coefficient appears to offer the most convenient and rapid determinations of diffusible hydrogen content.

14. SUBJECT TERMS

Steel, Weld Hydrogen Management, Hydrogen Trapping in Steel Welds, Retained Austenite, Hydrogen Sensors for Steel Weldments

15. NUMBER OF PAGES

45

16. PRICE CODE

17. SECURITY CLASSIFICATION OR REPORT	18. SECURITY CLASSIFICATION ON THIS PAGE	19. SECURITY CLASSIFICATION OF ABSTRACT	20. LIMITATION OF ABSTRACT
UNCLASSIFIED	UNCLASSIFIED	UNCLASSIFIED	UL

NSN 7540-01-280-5500

Standard Form 298 (Rev.2-89)
Prescribed by ANSI Std. 239-18
298-102

1.0 ABSTRACT

The development of methods to control the diffusible hydrogen content during high strength steel welding was performed. The perfection of the use of irreversible weld metal hydrogen traps was demonstrated. Efforts have effectively alleviated the available diffusible hydrogen, and thus the susceptibility of hydrogen assisted cracking, by the use of ferro-yttrium additions to the welding consumable. The range of welding parameter for the most effective use of yttrium as a hydrogen getter was determined.

The investigation of the influence of retained austenite on cracking susceptibility was also investigated. Issues regarding the amount of acceptable retained austenite and its tendency to release hydrogen upon changes of service temperature and stress were evaluated.

The development of an advanced measuring apparatus for diffusible hydrogen content based on electronic, optical, and magnetic property measurements was investigated. The effort is searching for a rapid and accurate determination for both diffusible hydrogen content and distribution. This investigation used the instrumentation acquired during the DURIP grant program. Optoelectronic property measurements of color shifts in WO_3, which was attached to the steel in the form of a thin film detector, have successfully measured the diffusible hydrogen content of higher strength steel hydrogen contents. Preliminary results have also illustrated that both magnetic property and thermo electric (Seebeck) coefficient measurements can also be used to assess hydrogen issues in steel. The Seebeck coefficient appears to offer the most convenient and rapid determinations of diffusible hydrogen content.

2.0 TABLE OF CONTENTS

3.0 INTRODUCTION

High strength low alloy (HSLA) steels are known to be susceptible to hydrogen cracking. As the strength increases, so does the risk of hydrogen assisted cracking (HAC) after welding. The hydrogen assisted cracking in HSLA steel welds is considered to take place when all the necessary conditions for cracking are satisfied simultaneously. These conditions include the combination of unacceptable diffusible hydrogen content, high restraint tensile stress, high hardness or a susceptible microstructure, and a temperature ranging between –50 and 100 °C (1, 2, 3). The main goal to make a HAC resisting high strength steel weldment is to reduce the amount of diffusible hydrogen. Common practice to reduce hydrogen cracking in high strength steel welding is the pre- or post- weld heat treatment. This practice is cost intensive and, in some critical cases, not effective. Alternative methods based on metallurgical principles have been studied both for technological and economic merits.

Irreversible weld metal hydrogen traps have been demonstrated to be effective in managing diffusible hydrogen content, and thus the susceptibility for hydrogen-assisted cracking. Ferroyttrium additions to the weld pool have significantly reduced the diffusible hydrogen content. The effort to fully characterize the influence of the welding parameters on yttrium transferability across the welding arc and on hydrogen trapping behavior in the weld deposition was performed. This information is necessary for a promising technological transfer from this R&D approach to the practical development of welding consumables.

The efforts to characterize and model the role of retained austenite in the higher strength steel weld metal in storing and supplying diffusible hydrogen, as well as to assess the associated issue of mechanical integrity was performed.

The successful efforts in developing a diffusible hydrogen sensor that increased the measuring efficiency by reducing test time and by allowing diffusible hydrogen testing were performed on the steel welds. Electronic property measurement techniques have shown that even further advances can be made for both rapid diffusible hydrogen content and distribution determinations associated with steel weldments. The Seebeck coefficient has been correlated to the diffusible hydrogen content in materials, allowing for very portable, but accurate, hydrogen measurements to be made on fabricated steel structures. The electronic property measurement equipment is now in place, resulting from our recent DURIP instrumentation grant received from the U.S. Department of Defense.

4.0 METHODS DEVELOPED AT CSM TO MINIMIZE HYDROGEN DAMAGE BY HYDROGEN MANAGEMENT

4.1 Fundamental Aspects of Hydrogen Trapping in Steel Weld Metal

Hydrogen trapping is a phenomenon where various microstructural features in steel have an attractive interaction with hydrogen. Such an interaction is originated due to the energetically favorable condition for hydrogen to reside in the trap sites rather than in the lattice sites. As depicted in Fig.1, the free energy of the hydrogen-steel system is lower as hydrogen atoms reside at the trap sites rather

than at the lattice sites. The attractive interaction can be quantified by the binding energy, which is the difference between the two free energy values shown in Fig.1 ($E_B = G_L - G_T$).

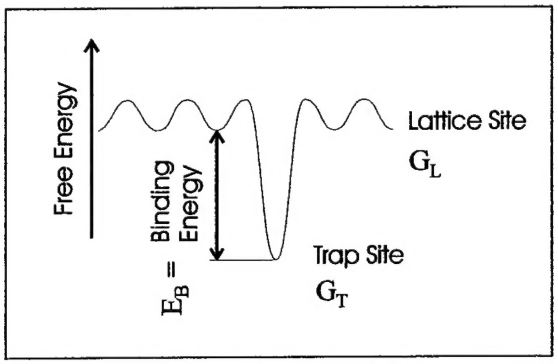

Fig. 1. *Illustration of energy levels for normal (lattice) sites (G_L) and trap sites (G_T).*

The binding energy between a trap site and a hydrogen atom causes a partitioning of the total hydrogen between the lattice sites and the trap sites. This partitioning can be calculated by means of thermodynamics principles and represented by the equilibrium fractional hydrogen occupation at the trap site, or hydrogen concentration at the trap site. The temperature dependency of the equilibrium fractional hydrogen occupation, ϕ_{eq}, follows the Fermi-Dirac statistics, according to Eq. (1)

$$\phi_{eq}(T(t)) = \frac{c_L \exp(-E_B / RT)}{1 + c_L \exp(-E_B / RT)} \qquad \text{Eq (1)}$$

where c_L, is the lattice hydrogen concentration, while R and T have their usual meanings. Temperature is denoted as $T(t)$ to emphasis its time dependency, considering a transient condition such as that in welding thermal cycle. In equilibrium conditions, c_L is equal to the solid solubility θ. The solubility equation reported by Quick and Johnson (4), which covers a broad range of temperatures (282 to 910 °C), was selected:

$$\theta(T(t)) = \frac{n_L}{N_L} = 0.00185\sqrt{P_{H_2}} \exp(-3440 / T(t)) \qquad \text{Eq (2)}$$

where pressure P is in atmosphere. For an open system, the variation of ϕ_{eq} with temperature, for various kinds of trap sites can be calculated, as shown in Fig.2. A trap with a high binding energy is capable to capture and to hold hydrogen atoms at higher temperatures than those traps having a lower binding energy. Hydrogen partitioning by a strong trap site occurs at high temperatures, during the course of welding cooling cycle. Such a partitioning can accelerate the reduction of diffusible hydrogen content in steel weldment, which therefore could minimize local accumulation of hydrogen at regions of stress concentration.

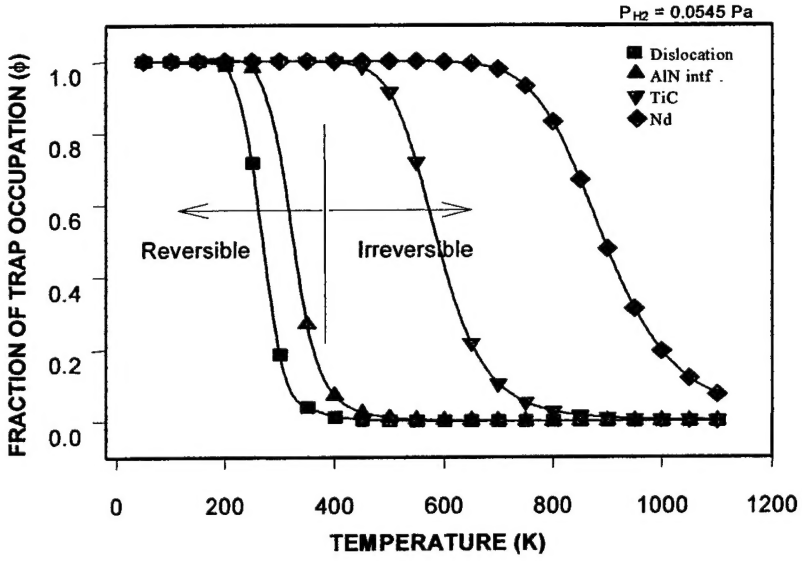

***Fig.2**. Equilibrium fractional occupation of hydrogen at trap sites, ϕ_{eq}. Calculations was done for atmospheric P_{H_2} = 0.0545 Pa. The binding energies for dislocation, AlN, TiC, Nd trap sites are 60, 65, 95, and 129 kJ/mol-H respectively.*

4.1.1 Theoretical Evaluation of Hydrogen Trapping

A theoretical study has been conducted to calculate the variation of diffusible hydrogen during welding thermal cycles, when trap sites are present in steel weld metal. With these calculations, the role of strong trap sites to expedite reduction of diffusible hydrogen without an extensive heat treatment can be theoretically explored. Variation of diffusible hydrogen was assumed to be a result of hydrogen degassing out of weldments, in addition to hydrogen trapping by a prescribed trap site. During a thermal cycle, diffusible hydrogen in a weld sample always reduces by degassing out of the weld sample, during either heating or cooling, until its content reaches the solid solubility at a temperature of interest. Diffusible hydrogen degassing out of the weld sample is governed by Fick's equation:

$$\partial c_L / \partial t = \nabla.(D \nabla c_L) \qquad \textit{Eq (3)}$$

There is a wide range of data for diffusion coefficients that have already been reported. The diffusion coefficients reported by Quick and Johnson (4) and by Nelson and Stein (5) is selected. In general, the diffusion coefficient follows the Arrhenius form of equation:

$$D(T(t)) = D_o \exp\left(-\frac{E_l}{RT(t)}\right) \qquad \textit{Eq (4)}$$

The simplest numerical solution of Eq. (4) has been derived by Pavlick et. al [2] as

$$dH_L = -\left(H_L - H_{eq}\right).D.K.dt \qquad \text{Eq (5)}$$

where, for rectangular shaped specimen $K = \left(\frac{1}{a^2} + \frac{1}{b^2} + \frac{1}{c^2}\right)\pi^2$.

The early mathematical model for hydrogen capture and release by a trap site is the McNabb and Foster equation (5):

$$\frac{\partial \phi}{\partial t} = \kappa c_L (1 - \phi) - \rho \phi \qquad \text{Eq (6)}$$

where, ϕ is the fractional hydrogen occupation or the hydrogen concentration at trap sites ($0 \leq \phi \leq 1$), c_L is the lattice hydrogen concentration (diffusible hydrogen), while κ and ρ are the capture and the release rate respectively. Following Oriano (7) $\rho = R^c \exp\left(-\frac{E_T}{RT}\right)$ with R^c and E_T as the release rate constant and the activation energy for hydrogen release respectively. Also, $\kappa = K^c \exp\left(-\frac{E_s}{RT}\right)$ with K^c and E_S as the capture rate constant and the activation energy for hydrogen capture respectively. E_S and E_T are related to binding energy E_B by the equation $E_T = E_B + E_S$.

During a welding cooling cycle, the hydrogen capture is the predominant interaction between hydrogen and the trap sites. In this study, Equation (6) was modified to establish the governing equation used for hydrogen capture during the cooling cycle. The mobility term was only represented by the capture rate ,$K^c.\exp(-E_S/RT)$, and driving force by $c_L.(\phi_{eq}-\phi)$, as written below

$$d\phi = K^c.\exp\left(-\frac{E_S}{RT}\right).\left(\phi_{eq} - \phi\right)c_L.dt \qquad \text{Eq (7)}$$

Inclusion of the equilibrium concentration of hydrogen at trap sites (ϕ_{eq}) in the above equation is to ensure that capture of hydrogen ceases when the actual concentration is equal or higher than the equilibrium concentration. The capture rate constant, K^c, was set equal to 100 lattice site/at H.sec and the activation energy for hydrogen capture, E_s, equal to the activation energy for hydrogen diffusion in the lattice (E_s= 7 kJ/mol).

A typical calculation of partitioning of hydrogen during a welding cooling cycle is shown in Fig. 3 for a trap site with a binding energy of 100 kJ/mol-H. An abrupt change of slope can be observed in the diffusible hydrogen content right after the martensite start temperature, M_s, of the weld metal. This abrupt change is because hydrogen transports in austenite and in ferrite are significantly different. In this study, Martensite start temperature was used to indicate phase transformation during the cooling cycle. The calculation should work as well for other transformation products, namely bainite and ferrite.

This model showed that the diffusible hydrogen content (c_L) of the weld metal containing traps is predicted to be lower than that of the steel without traps. The kinetics of hydrogen capture can be more clearly explained from Fig. 3.b., which shows the equilibrium trap occupancy (ϕ_{eq}), the actual trap occupancy (ϕ), and the rate of hydrogen capture ($d\phi/dt$). The hydrogen capture rate depends both on hydrogen diffusivity and the driving force for hydrogen capture ($\phi_{eq}-\phi$). It can be seen that a sudden increase in the rate of capture always follows the occurrence of martensite phase formation, where both capture rate determining factors are maximized.

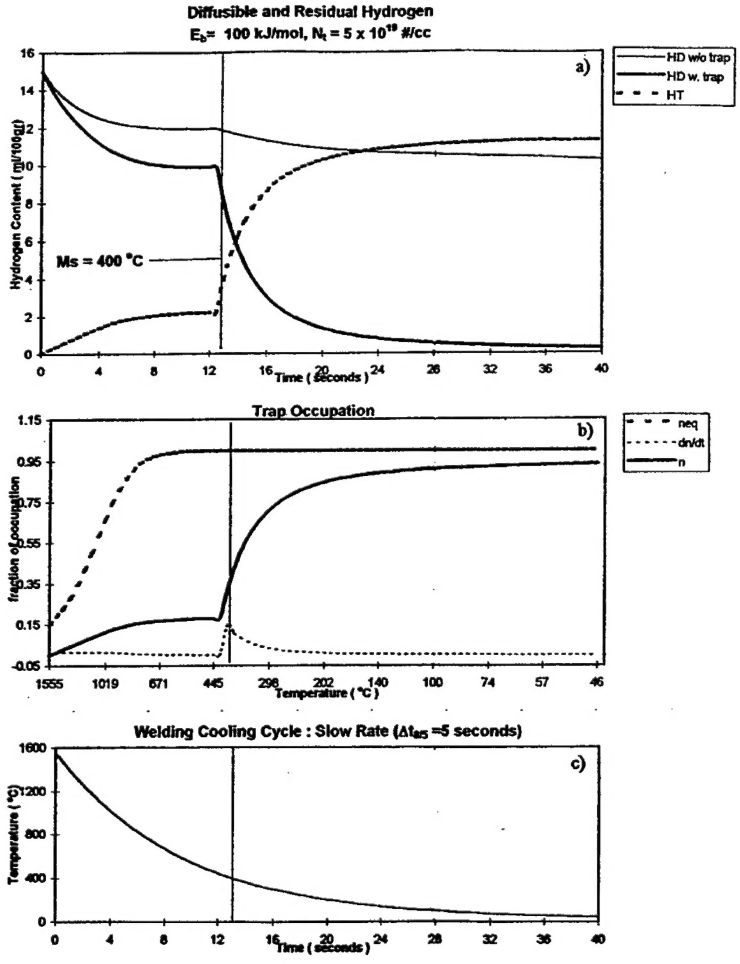

Fig. 3. Hydrogen trapping during welding cooling cycle. Initial diffusible hydrogen in weld metal is 15 ml/100g. In (a).,the notation c_L stand for diffusible hydrogen, c_T is the trapped hydrogen. In (b), ϕ is the fraction of trap occupation by hydrogen and ϕeq is the equilibrium fraction of occupation determined by the Fermi-Dirac distribution.

The model was developed to set a criterion and suitable conditions for the selection of traps that prevent HAC in high strength steel weldment. Proper trap additions should reduce the diffusible hydrogen rapid enough so that, during the cooling cycle, the diffusible hydrogen level at cracking susceptible temperatures (100-300 °C) is below the critical limit. The model demonstrates that this requirement can be achieved with proper combination of several factors such as martensite start temperature of the weld metal, trap-binding energy, trap concentration, and welding cooling rate.

The diffusion of hydrogen in the austenite phase is very slow, so that the hydrogen cannot be effectively captured or removed from the weld metal until the martensite temperature is reached. The lower the martensite start temperature, the more time is available for the hydrogen to remain in the weld metal interstitial sites. However, low martensite start temperature also means that the available temperature range for effective hydrogen diffusivity and trapping in the ferrite phase becomes narrower, and the suppression of diffusible hydrogen content trapping becomes less effective. The extreme situation is depicted in Fig. 4 for the case of weld metal possessing a martensite start temperature of 300 °C. The advantage of using a trap with higher binding energy, i.e., higher capture rate, is then obvious for this very narrow temperature range. However, the employment of high binding energy traps for a high martensite start temperature weld metal can lead to a situation where the trapping capacity will be wasted in high temperature regions. This behavior can occur even when the hydrogen diffusivity provides a high potential for easy hydrogen removal from the weld metal. Therefore, the selection of hydrogen traps must consider other factors than just the weld metal or consumable alloying contents.

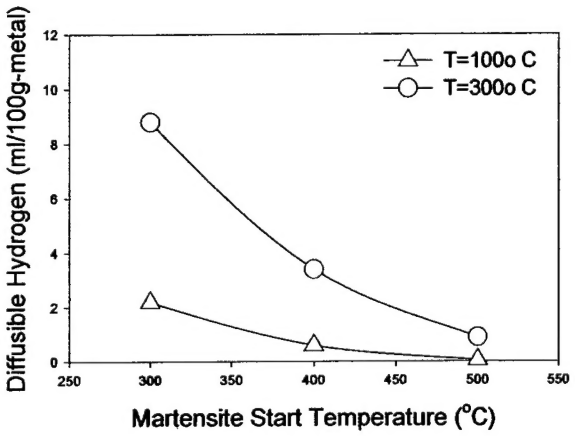

Fig. 4. Summary of diffusible hydrogen content at 100 and 300 °C during cooling cycle, as a function of martensite start temperature. Initial diffusible hydrogen content is 15 ml/100g-metal. E_B = 100 kJ/mol-H, $\Delta t_{8/5}$ is 5 seconds, trap density N_T= 600 at.ppm.

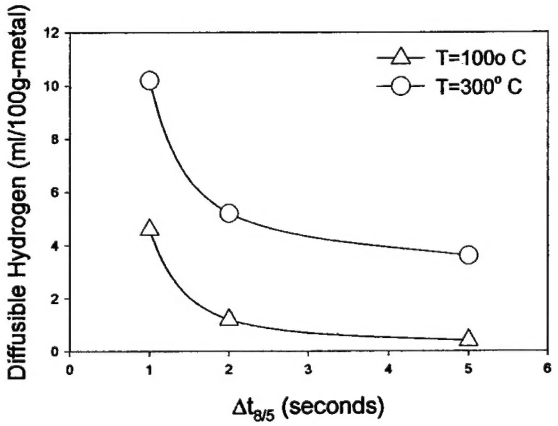

Fig. 5. Summary of diffusible hydrogen content at 100 and 300° C during cooling cycle, as a function of cooling rate ($\Delta t_{8/5}$). Initial diffusible hydrogen content is 15 ml/100g-metal. Ms = 400° C, E_B = 100 kJ/mol-H, trap density N_T = 600 at.ppm.

Conventional hydrogen management usually applies proper heat treatment or sufficiently low cooling rate to provide easy hydrogen removal from the weld and to form a microstructure resistant to HAC. In the case of weld metal containing trap sites, a certain rate of cooling is also necessary to allow sufficient hydrogen capture time before the temperature reaches 100 °C. In the present calculation, the cooling rate is assumed to occur naturally and relatively fast, so that sufficient hydrogen removal by lattice diffusion alone cannot be obtained. The effect of cooling rate, shown in Fig. 5, appears to be similar to that of the martensite start temperature. A very fast cooling rate, such as a rate with $\Delta t_{8/5}$ equal to one second, does not permit enough time for hydrogen to leave the weld metal or jump to trap sites. On the other hand, at a slightly slower cooling rate, the presence of traps

may yield a low diffusible hydrogen content at 100 °C and alleviate the tendency for weld metal HAC. This prediction shows the potential use of traps, substituting for the tight heat treatment procedure necessary for high strength steel welding.

In summary, a trap site should have a high binding energy to allow rapid hydrogen capture, especially in cases where the martensite start temperature is low. A high binding energy also minimizes release of hydrogen from trap sites during multi-pass welding. Depending on the concentration of trap sites and their binding energies, a minimum cooling rate, which depends on traps binding energy and trap density, is still required to achieve diffusible hydrogen content below the critical limit. However, this minimum cooling rate is still predicted to be faster than those rates of most conventional heat treatments used to prevent HAC in steel weld joints.

4.1.2 Hydrogen Thermal Desorption Analysis

Experimental evaluation of potential trap sites as well as assessment of their hydrogen trapping parameters can be done with hydrogen thermal desorption analysis. This measurement technique analyzes the release of hydrogen from various trap sites during a constant rate heating of the weld samples. The methodology applied in this analysis provides an easy way to evaluate a specific trap without excessive interference from other traps coexisting in the weld samples. As shown in Fig. 6 the apparatus comprises a temperature-controlled furnace and a fused silica tube wherein the weld sample is heated at constant rate heating and under constant argon carrier flow. The optimum argon flow through the fused silica tube, for the most heating rates applied, was found to be 10 ml/min. After leaving the fused silica tube, the sample gas (argon and hydrogen) is fed into a simple gas chromatograph for quantitative analysis. In the gas chromatograph, the gas sample enters the thermal conductivity detector (TCD). This detector produces a milli-voltage range output signal when a sample gas, with a different thermal conductivity than the carrier gas, passes through.

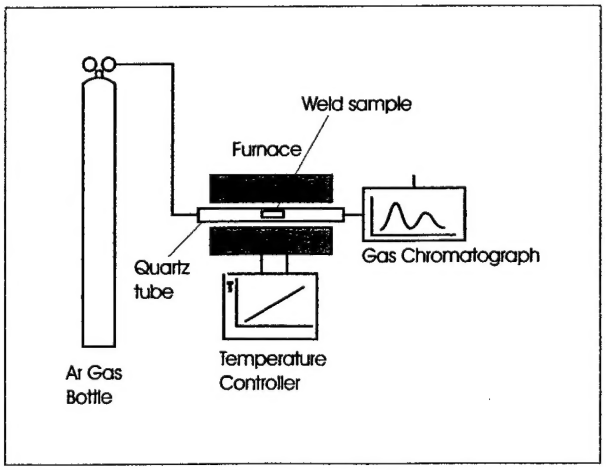

Fig. 6. Apparatus for the hydrogen thermal desorption analysis.

As simply explained by the Fermi-Dirac thermo-statistics, upon a heating process, hydrogen will be released from the trap sites with a rate dictated by the derivative of the fractional occupation of hydrogen with temperature, as shown in Figure 7. The desorption rate of hydrogen from a weak trap will have a peak at a lower temperature than that of a strong peak. A typical hydrogen desorption from commonly known weak traps in steel, such as dislocations and microvoids, is shown, for 4 °C/min heating rate and 2.5 mm thick AISI 1005 steel sample, in Figure 8. Dislocation and microvoids have a desorption peak around 150 °C and 400 °C, respectively. These peak temperatures are in good agreement with results reported by other investigators (8,9)

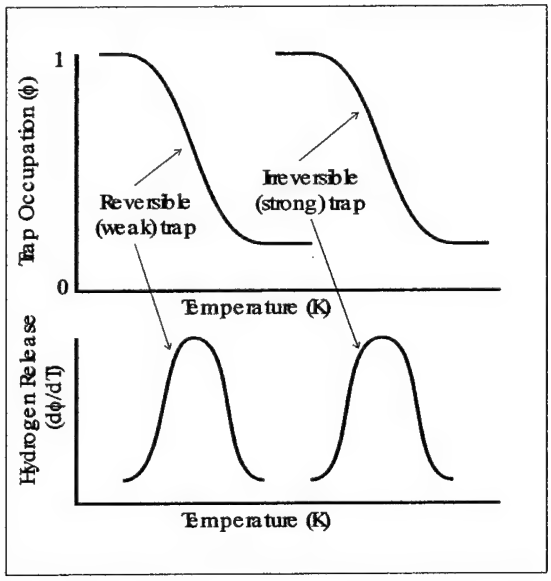

Fig. 7. Expected hydrogen desorption rate based on temperature derivative of the equilibrium fractional occupation of hydrogen at trap sites.

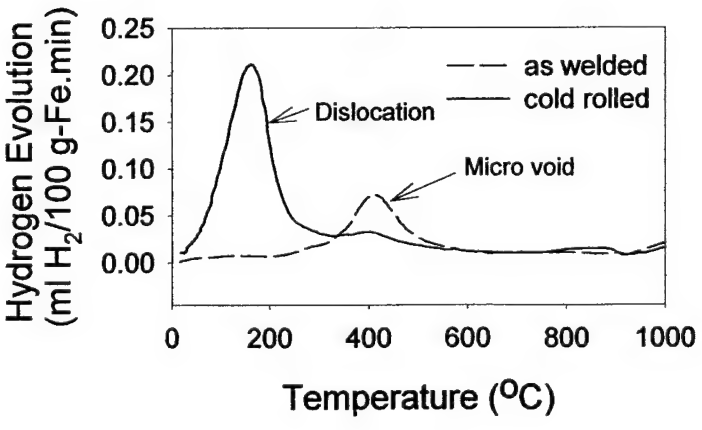

Fig. 8. Hydrogen thermal desorption of AISI 1005 steel (4 °C/min)

In order to trap hydrogen during welding cooling cycle, a strong trap has to be able to get to saturation high above 100 °C. From the equilibrium fractional occupancy, in Figure 2, the trap site has to possess a binding energy at least similar to that of AlN, which should have a desorption peak at least 500 °C, upon slow heating.

The hydrogen thermal desorption of yttrium containing high purity iron weld metal is shown in Figure 9.a., while that for HSLA 100 steel weld metal is in Figure 9.b. Also shown in these figures are hydrogen desorption of reference samples (Ref in Fig. 9.a and HSLA base in Fig. 9.b), which did not contain yttrium. Both hydrogen thermal desorptions were obtained after the measurement of diffusible hydrogen. They show the presence of hydrogen desorption with peaks at 600 °C and at 800 °C at 4°C/min (550 and 750 °C at 3°C/min). These desorptions indicate the presence of two kinds of strong trap sites in the weld metal. These desorptions also show that the reduction of diffusible hydrogen occurs because part of the total hydrogen was partitioned to the trap sites. Identification of the trap sites present in the weld samples with electron microscopy and X-ray diffraction analysis led the authors to a conclusion that the 600 °C desorption peak originated from Y_2O_3 inclusions and the 800 °C peak from Fe_2Y second phase. Details of the trap site identification are presented in another articles (10).

The hydrogen thermal desorption analysis has shown the high binding energy of the rare earth metal associated trap sites, as indicated by high desorption peak temperature. It also shows the potential use of the rare earth metal additions to provide accelerated reduction of diffusible hydrogen during welding cooling cycle. However, evaluation of these trap sites needs to be further pursued to assess the kinetics aspects of hydrogen release and trapping of these trap sites. The binding energy only relates to the driving force of the hydrogen capturing, but not the rate.

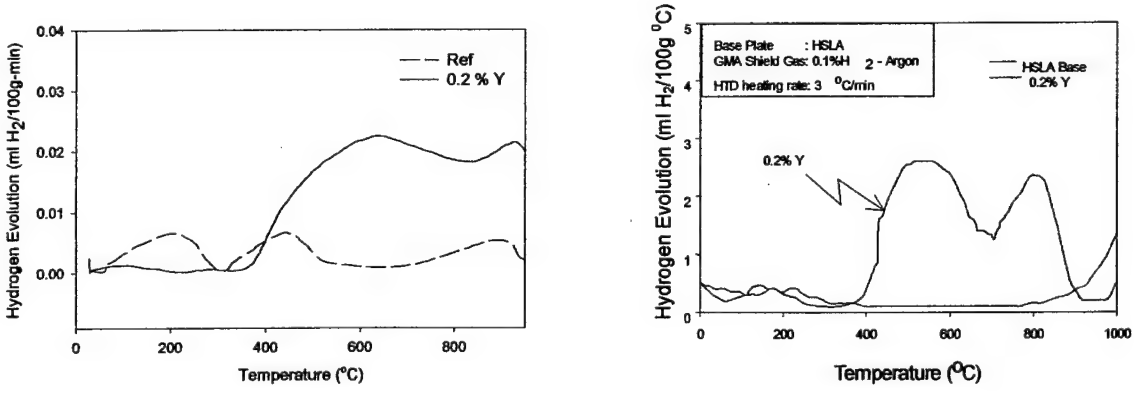

Fig. 9. *Hydrogen thermal desorption of weld metal GMA welded with 0.5 pct. H_2 in argon shielding gas and 600 ppm addition in the weld metal. (a). high purity iron base metal (4 °C/min) (b). HSLA naval steel base metal (3 °C/min).*

During heating, hydrogen release from trap sites is the predominant process. Hydrogen capture may actually occur but to much less extent. Therefore, for a heating cycle, hydrogen release is predominant and Equation (4) can be modified and simplified as written below

$$d\phi = R^c.\exp\left(-\frac{E_T}{RT}\right).\left(\phi - \phi_{eq}\right)dt \qquad \text{Eq (8)}$$

In the above equation, hydrogen release is governed by the mobility term $R^c.\exp(-E_T/RT)$ and the driving force $(\phi-\phi_{eq})$.

A typical result of calculated hydrogen desorption is shown in Fig. 10.a., for a steel sample containing two kind of trap sites, with their respective 60 and 100 kJ/mol-H binding energy. This calculation, for a 5 mm thick sample heated at 4 °C/min rate, assumed the same release rate constants for the two trap sites, which was equal to 100 sec–1. The activation energies for hydrogen release, for both traps, were assumed to be 10 kJ/mol higher than the corresponding binding energies. The hydrogen partial pressure in testing atmosphere was set equal to a common atmospheric value of 0.05 Pa (0.5 ppm). This calculation clearly shows that the peak of hydrogen desorption occurs at a higher temperature if the trap binding energy is higher.

Fig. 10.b. shows the variation of equilibrium ϕ_{eq} and actual ϕ hydrogen concentrations at trap sites with temperature. Unlike in Fig. 2, the equilibrium concentrations ϕ_{eq} was calculated based on the actual (supersaturated) lattice hydrogen concentration c_L, instead of hydrogen solubility θ, in Equation Eq *(2)*. There is a large temperature lag between the equilibrium concentration and the calculated hydrogen desorption. The temperature lag becomes larger if the hydrogen release rate constant R^c is smaller.

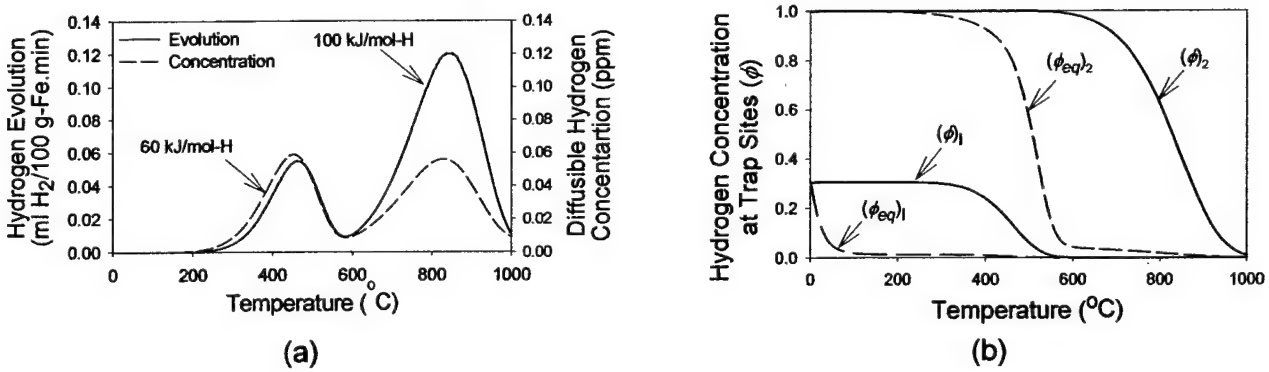

Fig. 10. *(a). Calculated hydrogen desorption of a steel sample containing trap sites with 60 and 100 kJ/mol-H binding energies. Heating rate at 4° C/min, rate release constant 100 sec^{-1}, 5 mm thick sample, and 0.05 Pa hydrogen partial pressure. (b).Equilibrium (ϕ_e) and actual (ϕ) trapped hydrogen concentrations during hydrogen desorption for trap I (60kJ/mol) and trap II (100kJ/mol). ϕ_{eq} was calculated with diffusible hydrogen content (c_L), instead of with hydrogen solubility (θ).*

4.1.3 The Search and Identification of Potential Trap Sites

Several researchers have proposed and explained the origins of hydrogen interaction with trap sites. One of the origins is elastic tensile stress field (11). Elastic tensile stress field is thought to be

the main origin of binding energy for dislocations and grain boundaries. Precipitates may also possess such an origin as a part of their binding energy, depending on the degree of coherency at their interfaces with the matrix. The rest of the values of binding energies, especially for precipitates and inclusions, originated form electronic interactions between hydrogen atoms and the trap sites. Troiano (12) gave one of the earliest explanations for such an electronic interaction. In his theory, the electrons of the hydrogen atoms will increase the electronic density state of the d bands of transition metals, increasing the repulsive forces between atoms. Any defect that introduces an electron vacancy in the iron d-shell electron level is thought to attract hydrogen to achieve local neutrality. For solute atoms in iron, attractive interaction with hydrogen will then exist when the impurity is located to the left of iron in the Periodic Table. On the other hand, solute atoms, which lie to the right of iron, will be characterized by repulsive interactions with hydrogen. Similar trends were also found for inclusions by Eberhart (13), using electronic structure calculations. Inclusions that contain transition metals far to the left of iron in the Periodic Table will be strong traps.

Experimentally, the above hypothesis for electronic interaction between hydrogen and trap sites can be demonstrated in the light of hydrogen thermal desorption analysis. Fig. 11 shows the hydrogen thermal desorption of AISI 1005 steel weld samples containing manganese and titanium respectively. The weld samples were prepared by using gas metal arc (GMA) welding and with addition of hematite (Fe_2O_3) powders. The addition of hematite was intended to as much as possible form oxides of manganese or titanium. The weld sample containing titanium released hydrogen at temperatures as high as 650 °C desorption peak, while the sample containing manganese did only up to 500 °C. This preliminary investigation demonstrated that titanium formed stronger hydrogen traps than manganese does. These results are in agreement with the hypothesis discussed above.

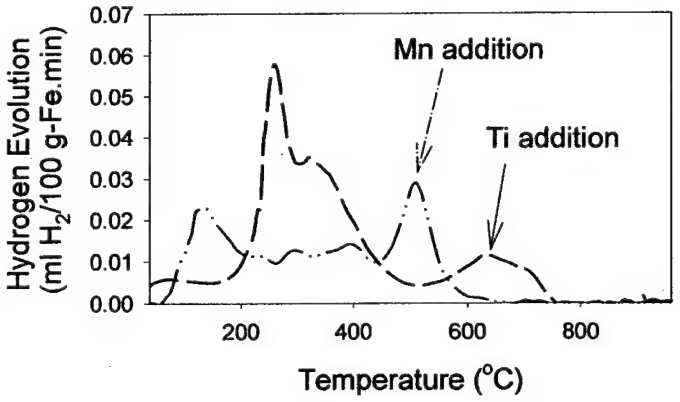

Fig. 11. *Hydrogen thermal desorption of AISI 1005 steel weld samples containing manganese and titanium, respectively (4 °C/min). The weld samples were GMA welded with addition of hematite powders.*

Titanium will certainly serve as a good candidate for a potential hydrogen trap site. Titanium carbide has been investigated by many researches and has been found to be a very strong trap site,

with a binding energy of 98 kJ/mol-H. On the other hand, titanium oxide, as the most probable form of titanium bearing inclusion in high strength steel weldment, has not been well investigated. Such an investigation will certainly beneficial for hydrogen management in high strength steel welding. Titanium also has a beneficial, but very sensitive, effect on the weldment mechanical integrity (14). Titanium oxide always reduces the Charpy impact transition; but a slight change in its content changes the transition temperature much more than some other oxides do. This change in transition temperature may indicate that slight change in titanium oxide content drastically change the weld microstructure. Among TiO_2, ZrO_2, Al_2O_3, CeO_2, and Y_2O_3 additions in welding electrode coatings, Y_2O_3 resulted the least change in the transition temperature. When added up 10 pct. additions, Y_2O_3 maintained a constant transition temperature of approximately –35 °C. Besides titanium oxide, yttrium oxide is the only oxide addition that did not increase the weldment transition temperature (14).

4.2 Rare Earth Metal Additions to the Weld Metal

An experimental study to investigate the role of hydrogen trapping, especially strong traps, in high strength steel welding was carried out by adding rare earth metal to the weld metal. These additions were made during gas metal arc (GMA) welding using metal-cored wires. The selected rare earth metals were neodymium and yttrium, which were inserted into the metal-cored GMA-wire consumables in powder form of iron-neodymium and iron-yttrium compounds, respectively. The powder size selected for the wire manufacturing was between -35 to -70 mesh.

Initial results were obtained from the measurement of diffusible hydrogen contents of the corresponding weld samples when GMA welded 0.5 pct. hydrogen contamination in the argon shielding gas. Welding parameters were adjusted for different wires to maintain a constant heat input of 1.5 kJ/mm. The diffusible hydrogen measurements were conducted according to the AWS specification (ANSI/AWS A4.3-93).

Figure 12.a. shows the amounts of diffusible hydrogen of samples welded with selected wire consumables, each resulting 150 ppm neodymium and 600 ppm yttrium addition in the weld metal. The result for high purity iron base plate and mild steel wire formulation demonstrated the expected reduction of diffusible hydrogen relative to a reference weld sample, which was free from such additions. Up to 50 pct. reduction in diffusible hydrogen by 600 ppm yttrium addition in the weld metal was obtained. The content of the elemental addition in the weld metal was measured by the inductance coupled plasma technique after digesting about 200 mg weld sample with concentrated acid mix.

Similar results were obtained when welding the same wires on HSLA 100 steel, as shown in Figure 12.b. Dilution of the alloying element from the HSLA 100 steel base plate was thought to reduce the transformation temperature from austenite to ferrite in the corresponding weld samples. As a consequence of the high solubility and the low diffusivity of hydrogen in austenite, higher content of diffusible hydrogen in the HSLA weld samples was apparent when compared to the high purity iron weld samples. However, the reduction capacity offered by 600 ppm. yttrium addition remained the same, which was 50 pct.

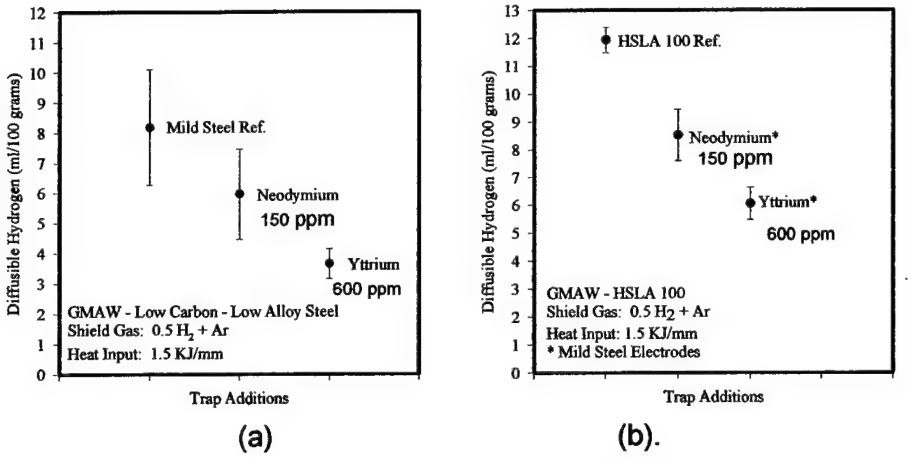

***Fig.12.** Diffusible hydrogen content of weld metal GMA welded with with mild steel formulated metal cored wires containing trap additions and 0.5 pct. H_2 in argon shielding gas. (a). high purity base metal (b). HSLA naval steel base metal.*

Further diffusible hydrogen measurements using only yttrium added metal cored wire are shown for two levels (1000 and 2000 ppm) of addition in Figure 13. This set of measurements also utilizes welding parameters which yields 1.5 kJ/mm but with 0.1pct. hydrogen contamination in the argon shielding gas. Figure 13 clearly shows the direct proportionality of diffusible hydrogen reduction with higher amounts of yttrium. Almost 90 pct. reductions can be achieved when welding with the wires that yield 2000 ppm in the weld metal. These results imply that addition of yttrium can be tailored to achieve a specific target value of reduction of the amount of diffusible hydrogen, as long as the other aspect of mechanical integrity of the weld joint is not severely affected.

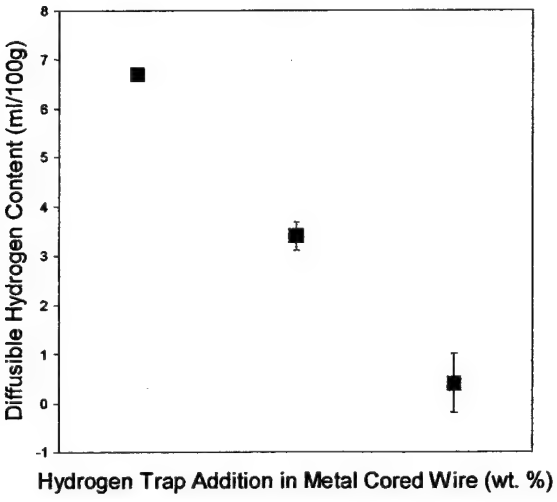

***Fig. 13.** Diffusible hydrogen content of HSLA steel weld sample GMA welded with mild steel formulated metal cored wires containing yttrium additions and with 0.1 pct H_2 in argon shielding gas.*

Diffusible hydrogen measurements have effectively demonstrated the potential use of a hydrogen trapping concept in the hydrogen management of high strength steel welding. However, this measurement cannot distinguish the performance of a strong trap site from a weak strong trap. The ice water quenching procedure stipulated by the AWS specification does not enable one to evaluate the hydrogen trapping performance of individual trap sites in the weld sample, especially above the critical hydrogen cracking temperature (100 °C). Any kind of trap will perform well in such a condition. The accelerated reduction of diffusible hydrogen that is expected from the use of a strong trap can not be evaluated by the simple diffusible hydrogen measurement.

An ideal measurement technique for this study would be a continuous measurement of degassed hydrogen from the weld sample immediately after the completion of the welding process. However, construction of such a system will have to wait until a more versatile hydrogen detectors are ready for field welding use (15).

Further evaluation of the rare earth metal additions was carried out in the light of hydrogen thermal desorption analysis. Hydrogen thermal desorption analysis was used to show that the reduction is directly associated with the hydrogen trapping of the rare earth metal additions in the weld metal. It also served the purpose of showing the strength of the trap sites in interest, as a direct indication of its capacity to provide accelerated reduction of the diffusible hydrogen.

Yttrium addition was investigated because it is possible that variation of yttrium oxide content in weldment does not drastically change the microstructure. If this situation is true, yttrium addition can be tailored to achieve certain target of diffusible hydrogen reduction. The same expectation is, of course, true for titanium. Other aspects of beneficial effects from yttrium addition in steel have been sufficiently investigated (16, 17)

Hydrogen thermal desorptions of selected AISI 1005 steel weld metals containing various densities of yttrium oxide are shown in Fig. 14. The reference sample (C) did not contain yttrium. The variation of yttrium oxide densities in the yttrium containing weld metals (A and B) was obtained by varying the oxygen content of the GMA welding shielding gas, while maintained the same level of yttrium addition. Sample A was welded with pure argon gas and sample B with 2 pct. oxygen and argon balance. Three distinctive hydrogen desorption peaks were identified, which are 420, 600, and 800 °C.

To identify the origin of the three hydrogen desorption peaks in Fig. 14, the three samples were analyzed for their x-ray diffraction patterns. As shown in Fig 15, sample C only exhibited the diffraction pattern of iron matrix. Sample A showed the intensities of bcc iron as well as Fe_2Y second phase. In sample B, the intensities of Fe_2Y second phase are reduced, while other intensities, which are belong to Y_2O_3, significantly emerged. A. Similar trend in amplitude variation was easily observed from the hydrogen desorption peak at 600 °C between the two samples. Briefly, it was concluded that Y_2O_3 release hydrogen at 600 °C and Fe_2Y does at 800 °C desorption peak temperatures. The peak at 420 °C was most probably originated from micro-voids.

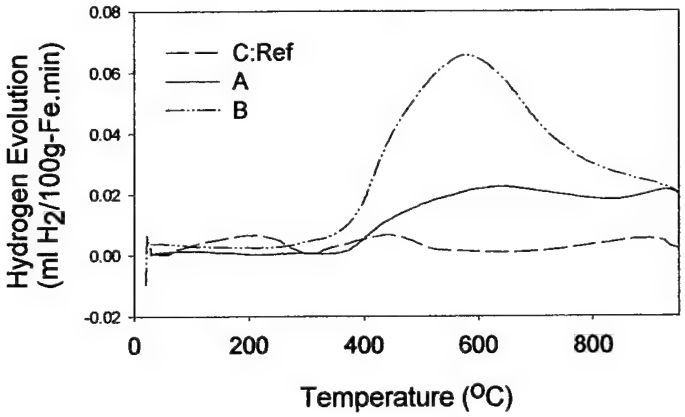

Fig. 14. *Hydrogen thermal desorption of selected AISI 100 steel weld metals containing various densities of yttrium oxide trap sites, starting from zero (C:Ref.), to roughly 50 pct. Y_2O_3 and 50 pct. Fe_2Y trap sites (A), and finally to roughly 75 pct. Y_2O_3 and 25 pct. Fe_2Y trap sites (B).*

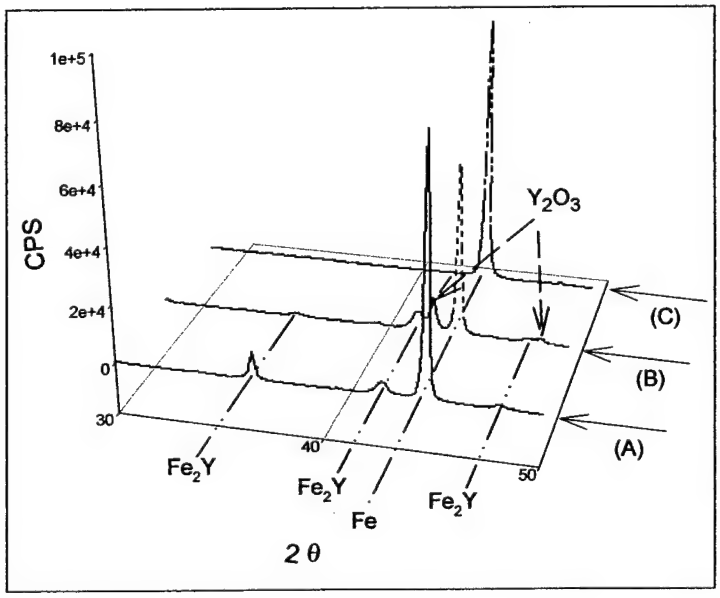

Fig. 15. *X-ray diffraction pattern from selected bulk AISI 1005 steel weld samples in Fig. 14: (A). sample A (50 pct. Y_2O_3 and 50 pct. Fe_2Y trap sites). (B).sample B (75 pct. Y_2O_3 trap sites), and (C) sample C:Ref*

The high desorption peak temperatures observed from the yttrium containing weld samples, indicated that these corresponding trap sites are strong hydrogen traps. To implement the use of these trap sites in the design of welding consumables and practices, their hydrogen trapping parameters have to be assessed. Even though Fe_2Y exhibited stronger trapping potential, further investigation focused only at Y_2O_3 because oxide is the more probable form that can be implemented in construction welding.

4.2.1 Assessment of Hydrogen Trapping Parameters

Kissinger's analysis (18) was used to obtain the activation energy for hydrogen release (E_T). The useful equation which was derived in this analysis is :

$$\frac{\partial \ln(\lambda / T_c^2)}{\partial (1/T_c^2)} = -\frac{E_T}{R} \qquad \text{Eq (9)}$$

where λ is the heating rate, and T_c is the desorption peak temperature. This analysis deduced the activation energy for hydrogen release, E_T, through the slope of an Arrhenius plot between $\ln(\lambda/T_c^2)$ and $(1/T_c)$. The Arrhenius plot was generated after recording the hydrogen desorption peak temperatures (T_c) of specific trap sites at different rate of heating (λ).

Five heating rates were applied to high purity iron weld samples containing yttrium to obtain sufficient data for the Arrhenius. Hydrogen desorption of the sample from three heating rates is shown in Fig. 16. The Arrhenius plot for each trap site in the weld sample is shown in Fig. 17.

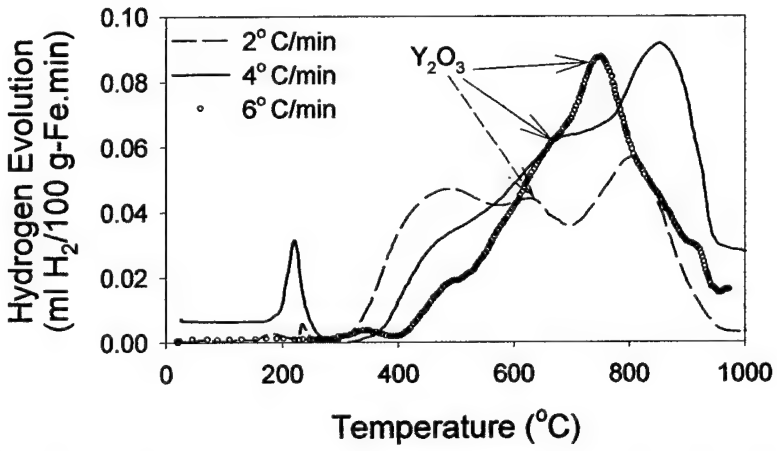

Fig. 16. *Hydrogen desorption of yttrium-containing high purity iron weld sample, for three different heating rates (2,4, and 6 °C/min)*

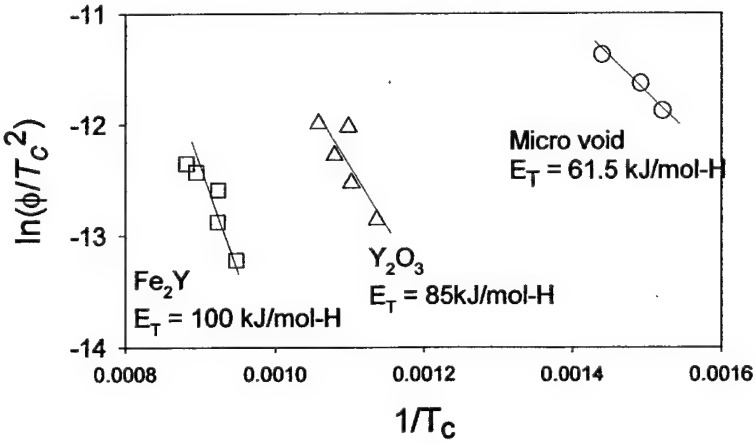

Fig. 17. *Arrhenius plot of ln (ϕ/Tc^2) versus $1/T_c$ for the trap sites present in the yttrium-containing high purity iron weld metal.*

An activation energy for hydrogen release (E_T) of 85 kJ/mol-H was obtained for Y_2O_3. This value was used as starting point for subsequent curve-fitting based on numerical solutions of Equations (5) and (9). The curve fitting was done for the actual hydrogen desorption curve of weld sample that was predominated by Y_2O_3 trap sites, namely sample B in Fig. 14. The curve fitting was performed to assess a more accurate value of E_T , as well as other hydrogen trapping parameters which affect hydrogen release during heating cycles. These parameters are the binding energy (E_B) and the release rate constant R^c. A lengthy procedure and criterion has been formulated to minimize the interdependency of these parameters in the curve fitting process. The best curve fitting, with the corresponding hydrogen trapping parameters is shown with the actual hydrogen desorption in Fig. 18. The fitted curve did not cover the left hand side of the hydrogen desorption because this side overlapped with hydrogen desorption of micro-pores. Similarly, the right hand side overlapped with the Fe_2Y desorption.

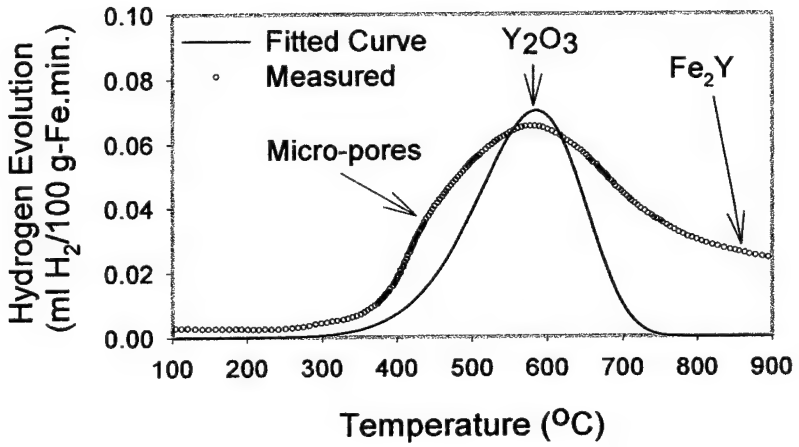

***Fig. 18.** Measured and calculated hydrogen desorption of Y_2O_3 trap sites in AISI 1005 steel weld sample, at 4° C/min heating rate (refined curve fitting). The calculation was done for E_T = 80 kJ/mol-H, E_B = 70 kJ/mol-H, and R^c = 60 sec^{-1}*

The remaining hydrogen trapping parameters to be found were those parameters associated with hydrogen capture. The activation energy for hydrogen capture, E_S, was easily deducted from the difference between E_T and E_B, which were already assessed (E_T=E_B+E_S). The final parameter, the capture rate constant (K^c), was obtained by selecting a sample that contained mostly Y_2O_3 trap sites (sample B in Fig.). The sample was hydrogen charged at one atmosphere partial pressure of hydrogen and at 350 °C, for different times from 10 to 150 minutes. After charging, the sample was rapidly heated up to 1000 °C, for a hydrogen desorption measurement. In this measurement all hydrogen desorption was assumed to be coming from Y_2O_3 trap sites. A reference sample (C in Fig. 14) was also treated identically to provide a background subtraction for noises, particularly that came from micropores. The amounts of hydrogen desorption were the area under the hydrogen desorption curves

Fig. 19 shows the amount of hydrogen desorbed during rapid heating for the selected sample and for the reference sample at different annealing time. The amount of hydrogen concentration at the Y_2O_3 trap sites were approximated by subtracting the area of desorption curves, obtained from the Y_2O_3 containing samples (sample B), with that area from the reference samples (sample C).

Mathematical description for the time dependence of hydrogen occupation at trap sites, such as that plotted in Fig. 20 can be derived by integrating Equation (9) with respect to time.

$$\ln(\phi_{eq} - \phi) = -K^c . \exp\left(\frac{-Es}{RT}\right) . c_L . t \qquad \text{Eq (10)}$$

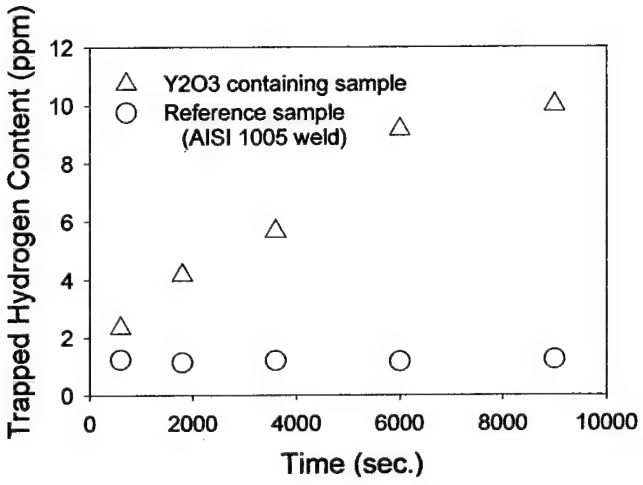

Fig. 19. *The amount of desorbed hydrogen during rapid heating cycle as a function of hydrogen charging time. Hydrogen charging was performed at 350 °C.*

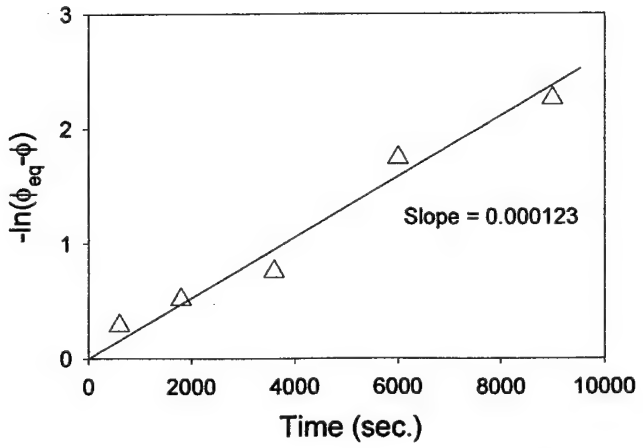

Fig. 20. *$-\ln(\phi_{eq}-\phi)$ plotted as a function of time. ϕ was the hydrogen concentration at Y_2O_3 trap sites obtained during rapid heating cycle.*

The values of the activation energy for hydrogen release, E_S, and the equilibrium concentration at trap site ϕ_{eq} (which is a function of binding energy, E_B), as well as hydrogen solubility, $c_L = \theta$, have been determined. Therefore, the last trapping parameter, the capture rate constant (K^c), can be deduced form the slope of $-\ln(\phi_{eq}-\phi)$ plotted as a function of time. At T = 350° C (623K) and p_{H2} = 1 atm., c_L was calculated to be equal to 2.45×10-6 (at.H/lattice site), ϕ_{eq} was 0.633, and exp(-*Es/RT*) was equal to 0.145. Assuming that hydrogen charging for 150 minutes saturated the Y_2O_3 trap sites up to ϕ_{eq} equal to 0.633, the variation of $\ln(\phi_{eq}-\phi)$ at Y_2O_3 trap site as a function of time can be plotted in Fig 20. The hydrogen capture rate constant K^c at Y_2O_3 was then found to be equal to 345 (lattice site/at H.sec). However, if c_L is expressed in at H/cm^3 iron, the capture rate constant K^c becomes 1.36×10^{-21} (cm^3/at H.sec).

In summary, the assessment of hydrogen trapping parameters for Y_2O_3 trap site is listed in Table 1. Quantitatively,Y_2O_3 is still considered a good candidate for the purpose of safe welding conditions from HAC, despite the fact that its binding energy is not extremely high. The relatively low value of activation energy for hydrogen capture (E_S), as well as high value for the hydrogen capture rate constant (R^c) would be more than enough to compensate the Y_2O_3 limitation in its value of trapping binding energy. One would better appreciate the potential of Y_2O_3 if its hydrogen trapping parameters can be compared with those of other inclusions. Unfortunately, only very limited numbers of investigators (19, 20) that attempted to assess complete information of such hydrogen trapping parameters. There are also many difficulties in this comparison because other investigators used different experimental techniques. In some cases, definition and basic assumptions of the trapping parameters differ among these investigators.

Table 1. Summary of hydrogen trapping parameters

Trap Sites	Y_2O_3
Activation energy for hydrogen release (E_T)	80 ± 5 kJ/mol-H
Binding energy (E_B) (minimum value)	70 ± 5 kJ/mol-H
Saddle point energy (E_S)	10 ± 5 kJ/mol-H
Release rate constant (R^c)	60 ± 10sec^{-1}
Capture rate constant (K^c)	345 ± 5 (lattice site/at H.sec) or 1.36×10^{-21} (cm^3/at H.sec).

4.3 Influence of Welding Parameters on the Hydrogen Trapping Effectiveness of Rare Earth Containing Welding Consumables (In Progress)

The development of welding consumables that introduce irreversible trapping elements into the weld pool to control the diffusible hydrogen has performed. This research has identified the effects of specific rare earth metal additions and demonstrated an ability to achieve very low weld metal hydrogen content, when introduced to weld pool in form of ferroaddition. Among these elements, yttrium was selected as the best candidate for trapping addition due to both its ease of manufacturability and its trapping irreversibility. Metal-cored wires with trapping additions have been made at CSM and have been evaluated for hydrogen control as function of the welding parameter. This work fully characterized the effects of voltage, current, travel speed, and polarity. As well as, the effects of oxygen levels on the yttrium transferability across the arc and on the resulting diffusible hydrogen content were investigated. Metal-cored steel wires containing various ferroyttrium contents were evaluated. Yttrium was found to form the oxide and/or yttrium oxy-sulfide in the weld metal, depending on the yttrium recovery and sulfur content. The metal transfer modes were observed and recorded during welding and mapped accordingly with the welding voltage and current as shown in Figure 21. Since hydrogen trapping as a time-temperature dependent process, it is essential to identify the welding process parameter space and which will allow for sufficient trapping without altering the steel weld metal properties. This work characterized the influence of the welding parameters on hydrogen trapping and defined the effective parameter range.

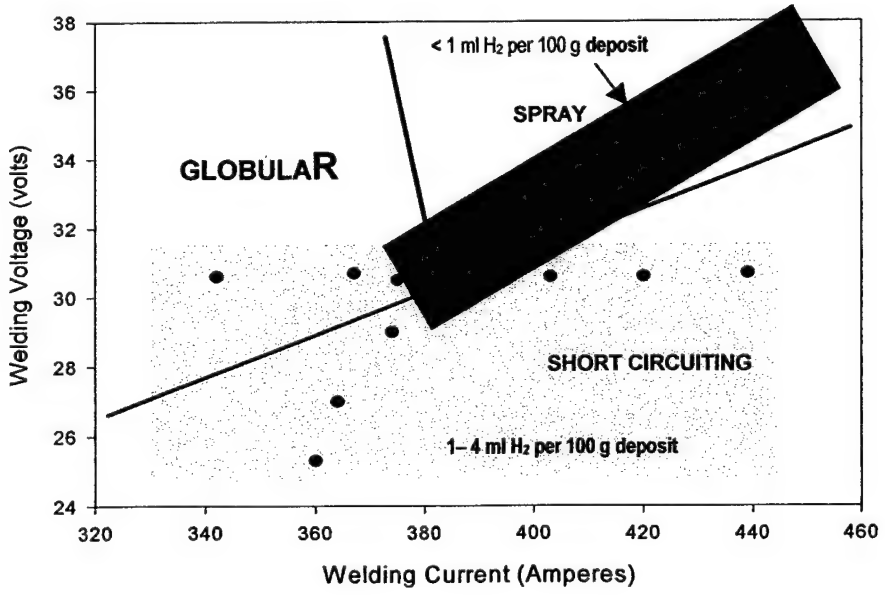

Fig. 21. *Metal transfer mode plot for gas metal arc welding with metal-cored wire.*

Gas chromatography was used to measure diffusible hydrogen contents of HSLA 100 steel welds according to the ANSI/AWS A4.3-93 standard. A range of heat input, from 1.4 to 3 kJ/mm, resulted a range of diffusible hydrogen content from less than one up to 4 ml of H_2/100 g weld deposit. As shown in Figure 21, an optimum operating window is shown for welds with less than one ml H_2/100 g. Within this window, the spray mode is the predominant mode. In the spray mode, yttrium is quite effectively transferred across the arc. Thermal desorption analysis showed that these yttrium containing weld metals have trapped the diffusible hydrogen irreversibly. This correlation will assist in making the best welding parameter selection for these new hydrogen trapping consumables.

4.4 Role of Retained Austenite in Hydrogen Management at High Strength Steel

Extensive investigations have been conducted in crucial role of microstructure in hydrogen assisted cracking in HSLA steel weld metal (13, 21). It has been suggested that martensitic microstructure is most susceptible in hydrogen assisted cracking in weld metal. However, the effect of retained austenite (or M/A constituent) on hydrogen assisted cracking has not been studied. Certain amount of retained austenite is inevitable in HSLA steel weld metal because of the thermal cooling cycle of welding. The resulting retained austenite exhibits a low hydrogen diffusivity and high hydrogen solubility. However, the surrounding microstructure of HSLA steel weld metal, which are mixture of ferrite, martensite and bainite, has high hydrogen diffusivity and low hydrogen solubility. These differences in hydrogen transport behavior between retained austenite and martensitic microstructure may result in retained austenite becoming a strong intraphase hydrogen trap, either temporary or permanently. Nelson (22) suggested that retained austenite can potentially be a continual hydrogen source to martensitic matrix through its life time. Hence, an understanding of the role of retained austenite on HAC is necessary to design hydrogen cracking resisting HSLA steel weldments and welding practices. Furthermore, retained austenite was an unstable microstructure, and may transform to martensite with changes in service temperature and applied plastic strain. In this event, hydrogen previously trapped in retained austenite may result in very high diffusible hydrogen contents available in the adjacent martensitic microstructure.

Some investigators (23, 24) clamed that hydrogen trapping in retained austenite can have beneficial role on hydrogen assisted cracking since austenitic microstructure act as a diffusional barrier to prevent hydrogen accumulation at crack tip. However, according to a previous investigation (25), TDA results for AISI type stainless steel and super duplex stainless steel suggest that this behavior is bulk hydrogen trapping, not a strong trapping between hydrogen and interfacial defects as shown in Figure 22. This result suggests that the retained austenite can be a reversible trapping site and have potential to easily become weak trapping site.

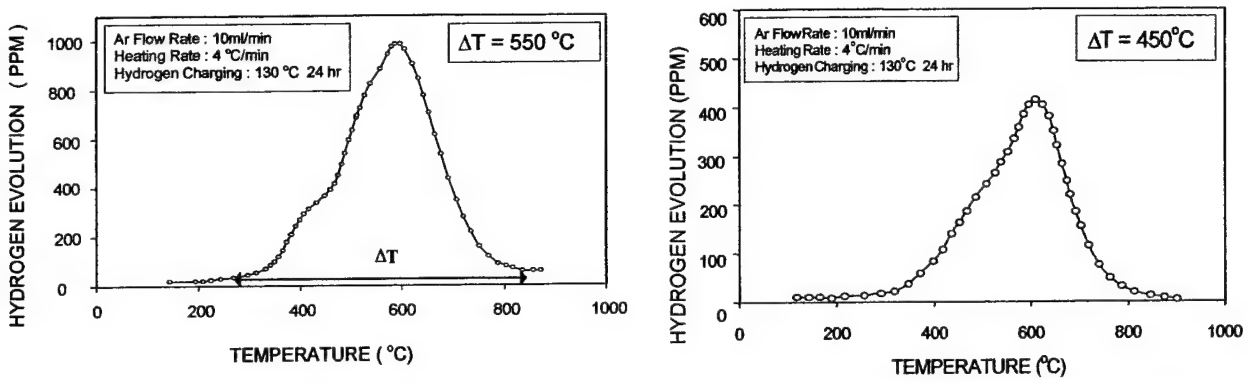

***Fig. 22-** Thermal desorption analysis results of AISI type 304 stainless steel and duplex stainless steel samples. The ΔT represents the hydrogen evolution temperature.*

Extensive investigations have been conducted in crucial role of microstructure in hydrogen assisted cracking in weld metal (26). It has been suggested that retained austenite microstructure could be detrimental to the hydrogen assisted cracking of high strength steel weld since hydrogen is much more soluble in austenite than ferrite. Particularly, it is more serious if they transform to martensite under stress or if some of the hydrogen is diffuse into adjacent martensite, which is well known as most susceptible in hydrogen assisted cracking in weld metal. However, the effect of retained austenite (or M/A constituent) in high strength weld metal on hydrogen assisted cracking has not been studied.

Previous investigation (27) revealed that retained austenite phase acts as strong hydrogen trapping site in dual phase steel (12 pct. retained austenite) and high strength steel weld metal. The TDA results are shown in Fig. 23 (a), (b). Since liquid nitrogen quenched weld metal sample has almost zero percent of retained austenite, no high temperature bulk austenite hydrogen peak is observed. By comparing two thermal desorption curves, it suggests that the hydrogen is released from much lower temperature since liquid nitrogen quenched weld metal does not have high temperature hydrogen trap. High solubility coupled with low diffusivity of hydrogen in austenite causes retained austenite to become supersaturated with hydrogen in the initial stage of cooling cycle. As a result, the potential for hydrogen assisted cracking is increased since surrounding microstructure (martensite, bainite or ferrite) has high hydrogen susceptibility. Also, Tsubakino *et al.* (26) confirmed that diffusion rate of hydrogen in high strength steel are influenced by the retained austenite which exists around bainitic ferrite plates. These studies suggest that hydrogen trapped in retained austenite will potentially have a continual source to martensitic matrix. Figure 24(a) shows the evolution rate curves of steel, which contains bainitic ferrite and 26 pct. retained austenite content. Figure 24(b) shows the evolution rate curve of type 304 stainless steel charged hydrogen. These results show that the curve corresponds to the release of hydrogen in retained austenite.

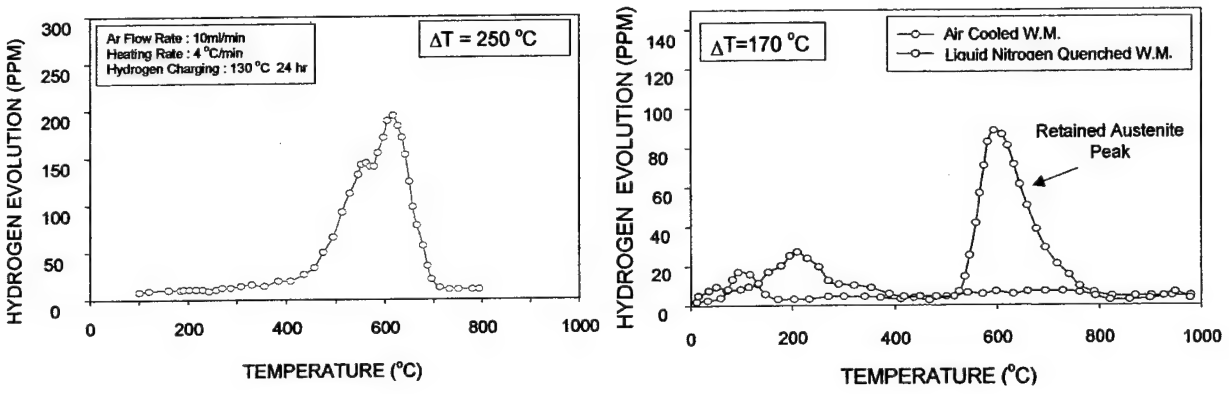

Fig. 23. Thermal desorption analysis of hydrogen charged (a) dual phase steel (b) HSLA steel weld metal

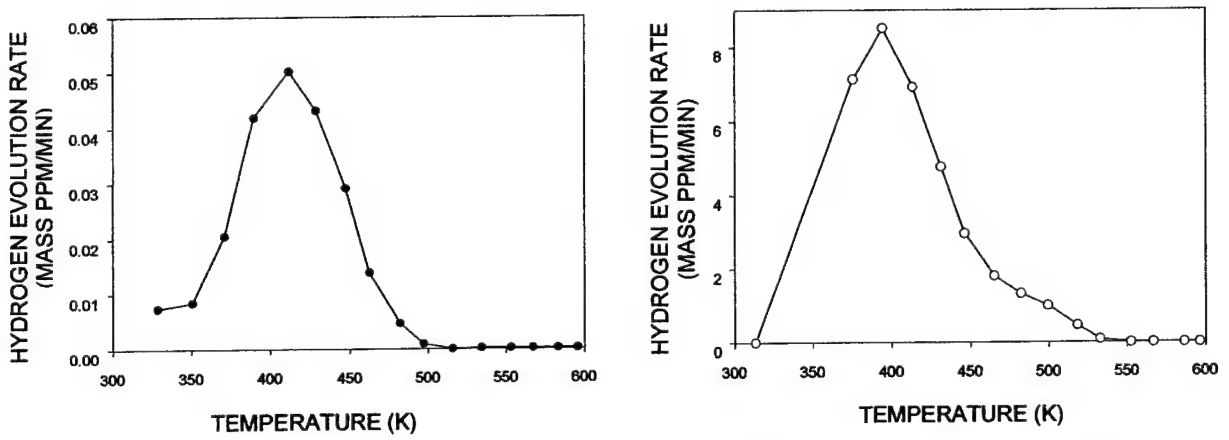

Fig. 24. (a) Hydrogen evolution rate curves in steel-12γ charged hydrogen for 173 and 684 ks. (*steel-12γ has 26% retained austenite) (b) Hydrogen evolution rate curve in type 304 stainless steel.*

The retained austenite stability is the other concern since it can transform to martensite under stress or low temperature. Prioul et al. (28) observed hydrogen effusion during the martensitic transformation and confirmed that hydrogen is mobile at subzero temperature during the martensitic transformation in nickel steel exhibiting burst transformation behavior. The hydrogen effusion during the burst is shown in Figure 25. They measured hydrogen effusion during cooling to 170K for nickel steel. According to the result, no effusion could be detected between 300 and 226K during cooling at 1.5 K/min. At 226K, a sudden release of hydrogen was observed. A previous investigation (25) revealed that martensitic transformation from unstable retained austenite changes trapped hydrogen transports behavior and may have significant effects on hydrogen assisted cracking since retained austenite can transform to martensite with changing in low service temperature and applied plastic strain. As a result of the hydrogen release from retained austenite microstructure, It is expected that the hydrogen is captured in weak traps. Dual phase steel was selected to observe the effect of retained austenite stability on hydrogen transport behavior.

Thermal desorption analysis was performed for dual phase steel samples, which were cold rolled 20 and 40 percent respectively as shown in Fig 26. The shifting of hydrogen evolution peak to the lower temperature for both samples was observed. In addition, the reduction of total amount of trapped hydrogen content was found. This situation was also observed in heavily cold rolled HSLA steel weld metal too. However, these cold rolled dual phase samples show more clear illustration of altering on hydrogen trapping phenomenon associated with retained austenite stability.

Since hydrogen trapping in retained austenite has significant effects on hydrogen assisted cracking in weld metal, it is suggested to reduce the susceptibility of cracking, by finding the strong irreversible trap in retained austenite which can stop hydrogen leaking from retained austenite to martensitic phase.

In real commercial applications, retained austenite transformation to martensite may occur when HSLA steel weldment is used in construction with severe cold condition. Also, when the HSLA weldments are experiencing cyclic loading, this condition leaves the residual strain inside of HSLA steel weldments. This residual strain drives a austenite to martensite transformation and a potential release of hydrogen.

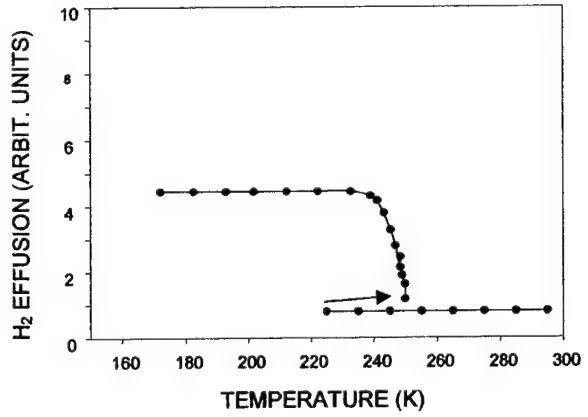

Fig. 25. Hydrogen effusion during the burst.

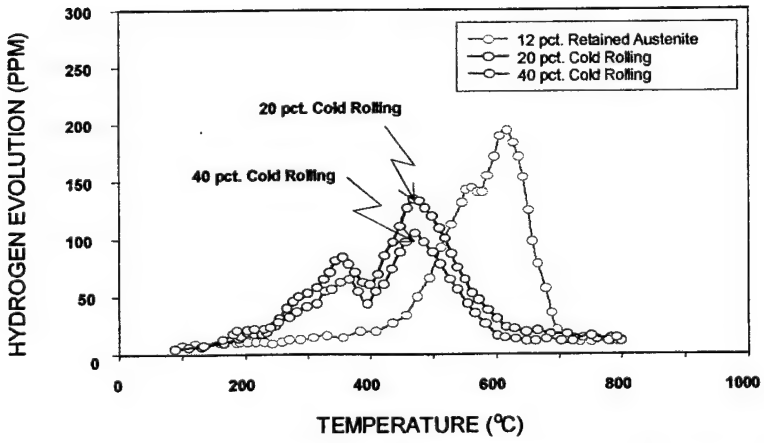

Fig. 26. Thermal desorption analysis of stress induced HSLA steel weld metal.

4.5 Accomplishments

4.5.1 Yttrium Control of Weld Metal Diffusible Hydrogen

Yttrium additions into the a low carbon steel have been found to make a major reduction in the weld metal diffusible hydrogen content and thus demonstrating the concept of weld metal hydrogen trapping by using irrepressible interfacial hydrogen traps. The interfacial traps were identified as yttrium oxide and/or a yttrium-Iron intermetallic phase. A major reduction of weld metal oxygen also occur during welding requiring careful control of the content of the yttrium addition to the welding consumable if the weld microstructure is not going to be significantly altered.

4.5.2 Influence of Welding Parameter on the Hydrogen Trapping effectiveness of Rare earth addition

The effectiveness of yttrium ferroadditions to the flux cored arc welding consumable on reducing the diffusible hydrogen content in higher strength low alloy steels has been studied. The range of current, voltage, travel speeds, and heat input used in welding were investigated using a systematic variation in their variable. The parameter range, including cooling rate, where yttrium allows effective management of the diffusible hydrogen was determined and reported. Careful control of the resulting weld metal oxygen is necessary to allow for the desirable optimum microstructure and properties.

4.5.3 The roles of retained austenite in hydrogen management of high strength steel weld metal

The thermal desorption analysis was employed to observe the hydrogen trapping and detrapping behavior of retained austenite in high strength steel weld metal. Retained austenite was found to be an intraphase hydrogen trapping site which has relatively high binding energy. This hydrogen trapping in retained austenite can increase the potential susceptibility of HAC in high strength steel weld metal. When the plastic strain and reduced temperature were applied on hydrogen charged specimens, the thermal desorption analysis exhibited a shifting of hydrogen peak to lower temperature. By applying different amount plastic strains, the retained austenite transforms to martensite and alters the hydrogen detrapping behavior. Quenching to liquid nitrogen temperature eliminates the existence of the retained austenite and no significant high temperature peak for hydrogen trapping was found. This result suggests that microstructural transformation associated with changes in service conditions may result in high diffusible hydrogen content in the resulting martensite phase. Also, the existence of retained austenite means an under-estimation of the amount of remaining diffusible hydrogen, when determined from standard diffusible hydrogen measurement. As a consequence, the common methods to predict safe welding conditions from HAC become too optimistic.

5.0 ADVANCED METHOD TO MEASURE DIFFUSIBLE HYDROGEN AND HYDROGEN DISTRIBUTIONS

With the increasing use of higher strength steels, the diffusible hydrogen content necessary to promote hydrogen assisted cracking (HAC) has become very small. This much lower diffusible hydrogen content level is approaching the uncertainty level of present diffusible hydrogen analytical practices, thus requiring the development of new analytical techniques. Efforts are being made to develop more sensitive and less time consuming methods for hydrogen.

Knowledge of the hydrogen distribution in a steel weldment, in addition to the nominal diffusible hydrogen content, is of primary importance for determining its susceptibility to hydrogen assisted cracking. Present methodologies to measure total and diffusible hydrogen are destructive and require excessive testing times. The present methods also do not produce information about hydrogen distributions and cannot be applied to a welded steel structure. This ARO project has focused on the development of new methods for quantitative analysis of hydrogen in welded steels that will determine both the content and distribution of diffusible hydrogen. The ultimate goal was to design a simple yet reliable method for on site determination of diffusible hydrogen content and distribution.

5.1 Present Welding Industrial Practice

In analyzing hydrogen in steels the distinction is made between total, residual and diffusible hydrogen. Diffusible hydrogen is considered to be mobile at lower (< 100°C) temperatures, whereas the remaining residual hydrogen is trapped in the metal. Total hydrogen is the combination of the two fractions. Residual hydrogen can be retained through interaction with microstructural discontinuities (24) or by the formation of hydrides with alloying elements.

Current methods for hydrogen analysis in welded steel therefore focus on measurement of the diffusible hydrogen content. The standard IIW method is the volumetric displacement of mercury (25-28). Results are reported as milliliters of hydrogen per 100g of deposited weld metal.

Other liquids including glycerin and silicone oil have been used for the test but have proven unsatisfactory. A significant drawback is the required analysis time. The test is time intensive, taking up to 72 hours to complete or up to twenty days for the IIW method (29).

A more modern method utilizing gas chromatography is also in use (30). Welded samples are placed in sealed containers and baked to release diffusible hydrogen. The evolved gases are transferred to a gas chromatograph. The gases are then separated with a packed molecular sieve column and analyzed with a thermal conductivity detector (TCD). The analysis (including sample preparation) takes up to 24 hours. The gas chromatography method gives comparable results to measurements in mercury.

5.2 Present Investigation and Accomplishments

This investigation consisted of three phases. In the first phase various advanced methods for hydrogen determination were considered. The methods for total hydrogen determination primarily

involved the use of laser ablation, where sample material was removed from the steel surface with a laser. The resulting evolved hydrogen was then measured using different types of detectors. For diffusible hydrogen determinations the hydrogen diffusing from the weld was captured directly and analyzed. The second phase of the investigation consisted of more detailed experiments on a suitable method determined in the first phase. This research led to the development of a diffusible hydrogen sensor based on the chemochromic reaction of certain transition metal oxides with hydrogen. The third phase investigated the use of electronic property measurements to determine the diffusible hydrogen content. The investigation attempted the use of the thermoelectric (Seebeck) coefficient to assess diffusible hydrogen content.

5.2.1 Phase I : LASER ABLATION METHODS

Non-uniform Distribution in Welds

The non-uniformity of hydrogen content can be attributed to differences between the weld and base metal microstructures (31, 32) and to strain gradients associated with the fusion line (33). The relative amounts of hydrogen in the weld metal and the heat affected zone are therefore a function of the compositional differences between the phases and can result in a non-uniform distribution. To the steel fabricator, this compositional difference is a strength issue of undermatch or over matching of the weld deposit relative to the steel plate.

Laser Induced Breakdown Spectroscopy (LIBS)

In this investigation, welded steel specimens were transported to Los Alamos National Laboratory to evaluate the technique of laser induced breakdown spectroscopy (LIBS) for the determination of total hydrogen. The specimens were analyzed and a hydrogen emission line at 656.2 nm was observed. A sharp increase in hydrogen was detected at the fusion line between the weld metal and the steel heat affected zone (HAZ).

The apparatus for laser induced breakdown spectroscopy (LIBS) has been described in detail elsewhere (34). The method uses a Nd/YAG laser to ablate the sample surface. The excited atoms in the laser plasma emit light of characteristic wavelengths. The emitted light is captured with a fiber optic cable and analyzed by emission spectroscopy.

The LIBS technique was successful in generating qualitative hydrogen distribution profiles in welded steel. However, quantitative reproducibility of the measurements was not satisfactory to establish an analytical practice for determining hydrogen distributions. It was therefore decided to investigate alternate methods of hydrogen detection while continuing the use of laser sampling.

Laser Ablation/Gas Chromatography (LA/GC)

Combining laser ablation (LA) with gas chromatography (GC) allowed for another analytical arrangement to measure hydrogen content and distribution. The use of gas chromatography has

already been accepted in the standard method for measuring diffusible hydrogen (35). A laser sampler is interfaced to the column of a gas chromatograph (GC). The sample surface is ablated with a laser. The evolved gases are swept into the GC using a stream of argon, which also serves as the carrier gas. The gases are separated in the column and analyzed with a thermal conductivity detector (TCD).

Although LA/GC was successful in quantitative differentiation of hydrogen levels in different areas of the weld, resolution was poor due to the long ablation times required to produce a detectable signal. Sensitivity could be improved by using a different detector such as a Pulsed Discharge Ionization Detector (PDD) with helium instead of argon carrier gas. A smaller customized sample chamber for maintaining samples at cryogenic temperature could also be incorporated. These improvements would undoubtedly increase the sensitivity of the method and possibly justify its use for total hydrogen determination.

Laser Ablation/Mass Spectrometry (LA/MS)

The principle of laser ablation was applied to the analysis of welded steels by the use of a mass spectrometer as detector. This technique has been used previously (36-44) on various materials including steel and titanium. Welded steel samples were ablated under high vacuum with a laser. The resulting gases were then transferred to a quadruple mass spectrometer that was optimized for hydrogen determination.

For these experiments, the samples were welded with deuterium gas in place of hydrogen. The deuterium therefore acts as an ideal tracer and minimizes signals from other contamination sources. Normally the separate detection of deuterium is difficult, but a mass spectrometer optimized for trace analysis of hydrogen can distinguish between the two hydrogen isotopes. A custom made vacuum chamber was constructed and mounted to the stage of a laser microscope. The chamber and microscope were located in a refrigerated cold room maintained at –32°C. The sample chamber could be viewed outside the cold room by means of a digital camera and the stage moved by remote control. The energy from a Nd/YAG laser was directed onto the sample surface using fiber optic cable. The evolved gases were transported directly into the sealed ion source chamber of a quadrupole mass spectrometer through 1.6 mm stainless steel capillary tubing.

The LA/MS technique was successful in generating qualitative hydrogen distribution profiles from welded steel. The data confirms the transformation theory of non-uniform distribution of hydrogen in welded high strength steels. The profiles imply that the compositional differences of the weld metal and base metal profoundly influence the final hydrogen distribution in the sample. The use of deuterium as a tracer assures that the signal is coming from the weld metal only and not from any other source. Of the methods investigated LA/MS is the most promising for the determination of total hydrogen distribution in welded steels.

5.2.1.1 Accomplishments of Phase I

The use of laser energy for determination of total hydrogen distribution in welded steel was investigated using various detection methods. Ablation of material from the weld surface allowed determination of hydrogen levels in different areas of the weld face. The small amounts of material removed necessitated the use of a sensitive detector. The presence of organic material on the sample surface posed problems due to surface contamination. For these reasons mass spectrometry was most suitable as a detection technique. The high sensitivity of the instrument and its ability to distinguish between isotopes led to the use of deuterium gas as a hydrogen tracer, which minimized signals from other sources than the weld. Further research will likely produce a useful laboratory method for quantitative determination of total hydrogen distributions. Based on these findings the following conclusions can be drawn:

1. Laser ablation/mass spectrometry (LA/MS) was determined to be the most suitable of the laser ablation methods investigated for analysis of total hydrogen distributions in welded high strength steels.
2. The use of shielding gas containing deuterium for welded samples analyzed with LA/MS allowed for a better understanding of the role of surface contamination.
3. Qualitative profiles generated using LA/MS confirmed the theory of non-uniform hydrogen distributions in welded steel as a function of differences in microstructural transformation.

5.2.2 Phase II: OPTOELECTRONIC DIFFUSIBLE HYDROGEN SENSOR

A sensor for measuring diffusible hydrogen content in welded steel which is based on the chemochromic reaction of certain transition metal oxides with hydrogen in air was investigated. The reaction is catalyzed by palladium or platinum, which adsorbs hydrogen on the surface and converts it to its atomic form. The hydrogen diffuses into the oxide and reacts to form an ion-insertion compound. The optical properties of the compound are altered and can be detected visually or spectroscopically.

The chemochromic (color change due to a chemical reaction) material used was a thin film of tungsten (VI) oxide, WO_3. For the purposes of hydrogen detection the gas must be able to freely penetrate the film. A porous, low-density film is therefore desirable; evaporative deposition provides films with these properties.

The reaction of hydrogen and WO_3 in air is represented by the equations

$$Pd + xH_2 + x/4O_2 + WO_3 \leftrightarrow H_xWO_3 + x/2H_2O + Pd$$

$$h\nu + W^{5+}(A) + W^{6+}(B) \rightarrow W^{6+}(A) + W^{5+}(B).$$

The reaction of WO_3 with hydrogen in the presence of a catalyst is well documented and sensors have been previously devised for detecting hydrogen (45, 46). The same concept was applied to detection of hydrogen evolving from the weld metal of high strength steel samples. The response of

the sensor to hydrogen diffusing from a weld was investigated by using a sensor housing designed for attachment to the welded specimen. The results indicated that the amount of hydrogen diffusing from the weld deposit was more than adequate for detection. the response curves the hydrogen from the weld deposit was still detectable by the sensor after a period of five hours.

For these experiments HSLA 100 steel was gas metal arc welded using levels of 0.1, 0.5, 1.0 and 3.0 pct. hydrogen in argon shielding gas. The specimens were welded in duplicate; one set of specimens was analyzed by the standard gas chromatography (GC) method to generate and report the results in ml/100 g weld metal. The other set was analyzed using the sensor.

From the signoidal shape of the response curves, it was decided to attempt and correlate the slope of the curve to the initial concentration in the specimen. The steady state portion of the curve could be assumed to be proportional to the flux of hydrogen from the weld metal. To investigate this possibility theoretical curves were generated using an equation derived from the error function erf(x). The diffusion was assumed to occur from a semi-infinite plane sheet with a uniform initial concentration C_o throughout and a constant surface concentration of zero. Solutions were generated for different initial concentrations as a function of time.

The slope of the response curve for each specimen was then calculated and converted to the same units using the calibration curve. The correlations were achieved between the GC results and the slopes of the sensor response curves, as well as with the theoretical curve derived from the diffusion equation. A statistical analysis was performed on the data set, and the residual standard deviation for the curve was found to be $\pm$ 0.00865 µl/min and had a correlation coefficient of 0.989.

The fit to the theoretical data is quite good, especially when the non-uniformity of the weld deposits is taken into account. These results indicate that the sensor could be used as an analytical tool for diffusible hydrogen measurement in welded steel. A further modification could incorporate an array of fiber optic sensors for determination of diffusible hydrogen distributions across the weld from traditional type diffusible hydrogen specimens.

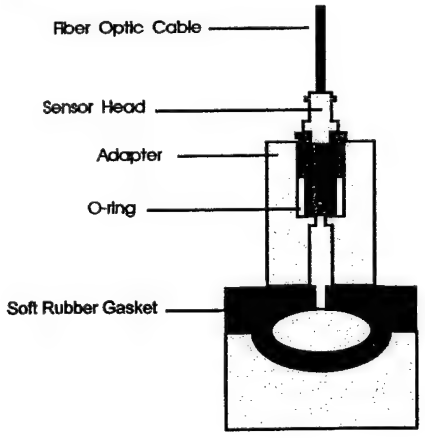

Fig. 27. *Design for prototype diffusible hydrogen sensor.*

The configuration of the sensor consists of a rubber gasket seal that conforms to the curvature of the weld bead (Figure 27). The gasket is attached to a sensor assembly, which consists of a small

enclosed volume to capture evolving hydrogen from the weld metal surface, as well as an enclosure for a fiber optic cable. The cable is coated with a gasochromic material (WO_3 thin film) that undergoes a color change in the presence of hydrogen gas. The hydrogen must pass through a palladium catalyst to produce atomic hydrogen, which goes into the thin film. The change in the reflected light from the coating is proportional to the hydrogen concentration inside the sensor volume.

To correlate the concentration of hydrogen desorption in the sensor to the initial diffusible hydrogen in the weld metal, the rate of hydrogen desorption is measured and adjusted for the surface area sampled. With the known diffusion coefficient of hydrogen in the steel weld, the initial concentration in the steel can be determined with an equation derived from the error function solution (47). A calibrated sensor will yield a response curve with the slope of the curve proportional to the diffusion rate, as shown in Figure 28. This rate can then be used to directly calculate the initial hydrogen concentration.

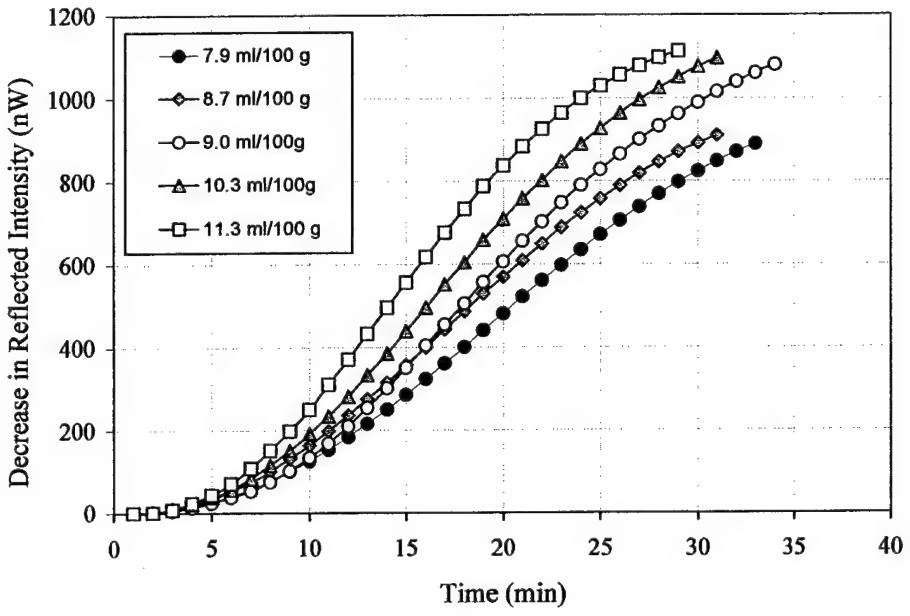

Fig. 28. *Experimental hydrogen response curves for diffusible hydrogen sensor (gas metal arc welded HSLA 100 steel.)*

The primary advantage of this sensor is its ability to measure actual welds on structures. Arrays of sensors can be used to monitor hydrogen along the entire length of the weld with emphasis on high stress areas. The other major advantage is lower cost. The analysis takes considerably less time than traditional methods, only 30 min compared to 48 to 72 hrs by traditional mercury or chromatographic techniques. The sensor itself is relatively inexpensive and could be made disposable. The major cost for the sensor is the electronics required for collecting and processing the optical data. This sensor has been described previously (48-50).

5.2..2.1 Accomplishments of Phase II

1. An optoelectronic diffusible hydrogen sensor has been developed. The sensor generates results quickly, and allows analysis of an actual welded structure as opposed to a laboratory specimen.
2. The sensor has been calibrated to yield quantitative results in ml/100 g weld metal as a function of hydrogen diffusion rates from the sample surface. A resulting effective diffusion coefficient of 7.5 x 10^{-5} cm^2/sec provides a good fit to measured data.
3. A patent application entitled "Method and Apparatus for Determining Diffusible Hydrogen Concentrations, NREL Patent #ProV/99-03 (2000)" was submitted.

5.2.3. Phase III: Seebeck Hydrogen Instrument to Determine Diffusible Hydrogen Content and Distribution

5.2.3.1. Nature of Hydrogen in Transition Metals

The nature of hydrogen in an alloy can be related to both solution thermodynamics and solid-state physics concepts. The heat of mixing of hydrogen in the metal carries information as to whether an alloy is a major hydride former or whether the hydrogen is in solid solution. Hydrogen as an electron acceptor or donor can be correlated to whether a specific material has a hydride-forming tendency or hydrogen solubility behavior.

Figure 29 illustrates the electron distribution for three cases (51). The left diagram is the electronic distribution for a transition metal with no absorbed hydrogen. The middle diagram is for a transition metal or alloy with electron donation from hydrogen absorption, with donated electrons primarily in the d bands. The right diagram illustrates donations to the d band, as well as some electrons becoming localized within the s, p band, causing the formation of a metal hydride. The right diagram exhibits the desired behavior for a hydrogen storage electrode for a reversible battery.

The hydrogen interaction with a typical ferrous weld can be modeled with concepts illustrated in the middle diagram.

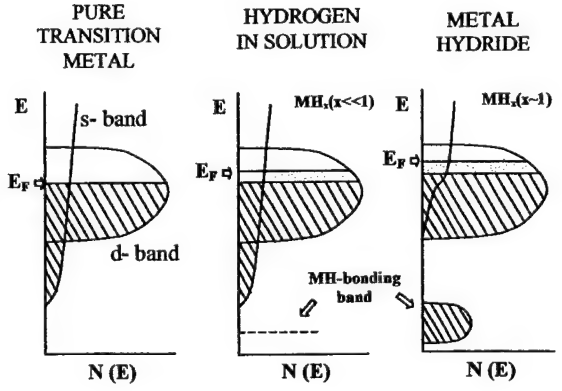

Figu.29. *Electronic structure of hydrides (52).*

In a solid solution made up primarily of those elements to the right of the middle of the transition metal series, the hydrogen atoms give their electrons to the d band and thus become mobile as protons in the lattice. This model agrees with most of the recent understanding of hydrogen transport in steels. This alteration of the d band can change the magnetic susceptibility and, vice versa, the magnetic field can alter the filling of the d states in such a way as to alter the solubility of diffusible hydrogen. These findings suggest that ferromagnetism could potentially influence the susceptibility to hydrogen-assisted cracking.

The functional connection between the content of diffusible hydrogen and magnetism can be seen from two separate definitions of ΔG, the Gibbs free energy. The Gibbs free energy was defined as an energy operator to describe the external work. For chemical equilibrium which has no external work, $\Delta G = 0$. For electrochemical equilibrium, $\Delta G = -n\,F\,E$, where $n\,F\,E$ is the external work, with n equal to the number of moles of electrons transferred by the half cell reaction, F is the Faraday constant, and E is the electrochemical potential.

For a system experiencing a magnetic field, the external work will be $\Delta M\,B$ where ΔM is the change in magnetization and B is the magnetic flux density. It follows that a metal-hydrogen reaction, such as

$$H_2 \rightarrow 2H, \qquad \textit{Eq (11)}$$

can be described by the equation relating ΔG to the activities:

$$\Delta G = \Delta MB = \Delta G^{\circ} + RT \ln \frac{[H]^2}{[P_{H_2}]} \qquad \textit{Eq (12)}$$

where ΔG° is the standard state free energy of the reaction for equation (11), $[P_{H_2}]$ is the partial pressure of hydrogen in equilibrium with the hydrogen in the metal, and $[H]$ is the equilibrium hydrogen content in metallic solid solution. It is apparent that change in the diffusible-hydrogen content $[H]$, can alter the magnetization ΔM.

The Gibbs free energy is also defined as

$$\Delta G = \Delta H - T\,\Delta S \qquad \textit{Eq (13)}$$

where ΔH is the heat of solution for hydrogen in the metal, and ΔS is the entropy, which can be defined by Boltzmann's expression,

$$\Delta S = k \ln W \qquad \textit{Eq (14)}$$

where k is Boltzmann's constant and W describes the availability of sites for the hydrogen. For transition metals, where the hydrogen atom donates its electron to the d band, the donated electron alters the electron spin configuration and thus the material's response in a magnetic field. The changes in electronic configuration in the d band can alter ΔS and thus ΔG, resulting in a change $\Delta M\,B$.

From a negative value on the left side of the first row of the transition metals in the periodic table, ΔH increases in value as one proceeds across to approximately manganese, where ΔH becomes positive. A negative ΔH suggests that hydrogen is an acceptor of an electron from a metal atom, causing localization of the electrons between the metal atom and the hydrogen, and promoting

the formation of a metal hydride. As ΔH approaches zero and becomes positive, the hydrogen-metal interaction is one of hydrogen solubility. This hydrogen solubility is the result of hydrogen becoming an electron donor to the d band. This electron donor behavior allows the electronic and magnetic measurements to be correlated to the diffusible hydrogen content of the metal. Each transition metal or alloy will have its own specific characteristic range for change in magnetization with variation in the diffusible hydrogen content, but for that characteristic range it should correlate and standardize to the diffusible hydrogen content measurements.

5.2.3.2 Electronic Sensor For Hydrogen

The thermoelectric power coefficient (Seebeck coefficient) is determined from the ratio of the temperature difference and voltage. This coefficient is an intrinsic property of a material. A simple and flexible experimental apparatus consists of two massive copper probes maintained at different temperatures measured with thermocouples mounted in the probes (Figure 30). The potential difference is measured across the two copper probes. Good electrical and thermal contacts were provided between the sample surface and probes. The absolute thermopower (Seebeck coefficient) of the alloy material S_a can be determined from measurements as

$$S_a = \frac{V}{\Delta T} - S_{Cu} \qquad \textit{Eq (15)}$$

where V is the Seebeck voltage measured between probes, ΔT is the temperature difference, and S_{Cu} is the well-calibrated Seebeck coefficient for copper. One of the blocks was maintained at room temperature and the other one at a temperature higher by 5 to 10 °C. The correlation of the Seebeck (thermoelectric) coefficient to the alloy hydrogen content allows a probe with two surface contacts to make a nondestructive hydrogen analysis of welds in fabricated structures.

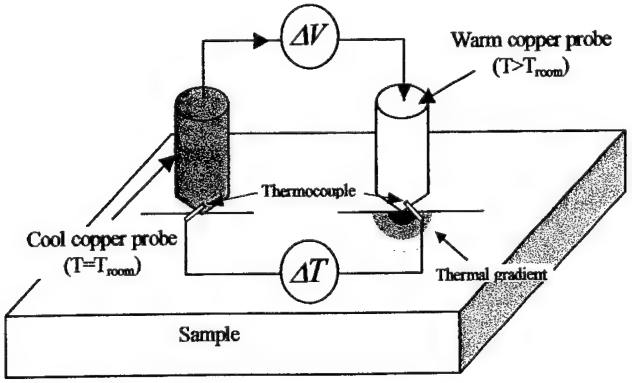

***Fig. 30** – Schematic sketches of the thermoprobe type Seebeck measurement.*

The Seebeck coefficient's value and sign in metallic alloys depend on the electron spectrum features in the vicinity of the Fermi level, such as the effective mass tensor, density of electronic states, and dominating scattering mechanism. In turn, the Fermi energy value (Fermi surface in k-space) changes with the change of electronic filling of the conduction band caused by the electron donation by the hydrogen atoms.

For example, for the parabolic spherical band and high degeneracy of the electron gas, the resulting Seebeck coefficient, S, is related to electron theory through the following expression, which holds for high carrier concentrations and $(E_f-E_o)/kT > 5$;

$$S = \left(\pm\frac{k}{e}\right)(27.1)\left(r+\frac{3}{2}\right)\left(\frac{m_e}{h^2}\right)\left(kTn^{*\left(-\frac{2}{3}\right)}\right) \qquad \textit{Eq (16)}$$

where r is the scattering parameter determined by the dominant scattering mechanism, h is Planck's constant, k is Boltzmann's constant, n^* is the free electron concentration, and m_e is the effective mass (51). From the free electron model, the electron concentration is directly related to the Fermi energy, and the effective mass describes the rate of filling of the energy states in k space at the Fermi energy level with increasing electron concentration. The effective mass can be described as:

$$m_e = \hbar^2\left(\frac{d^2E}{dk^2}\right)^{-1} \qquad \textit{Eq (17)}$$

where k is the wave vector. The effective mass, m_e, describes the shape of the s, p, d bands that are in contact with the Fermi energy level. The shapes of the bands at the contact position offer a characteristic indication that can be measured with changes in the Fermi level due to electron donation from the hydrogen content.

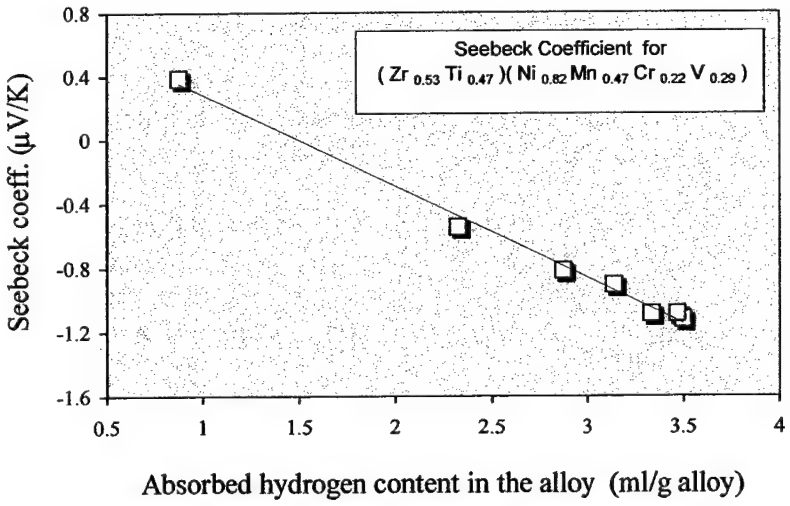

Fig. 31 *The variation of Seebeck coefficient with the amount of hydrogen stored in* $(Zr_{0.53}Ti_{0.47})(Ni_{0.82}Mn_{0.47}Cr_{0.22}V_{0.29})$.

Figure 31 illustrates the variation of the Seebeck coefficient with variations in the hydrogen content in hydrogen AB_2 storage alloy: $(Zr_{0.53}Ti_{0.47})(Ni_{0.82}Mn_{0.47}Cr_{0.22}V_{0.29})$. Similarly, Figure 32 illustrates the changes in the Seebeck coefficient with variations in diffusible hydrogen content in Invar (Fe–36Ni alloy). The linear correlation makes the Seebeck coefficient measurement very convenient and sensitive for assessing diffusible hydrogen content.

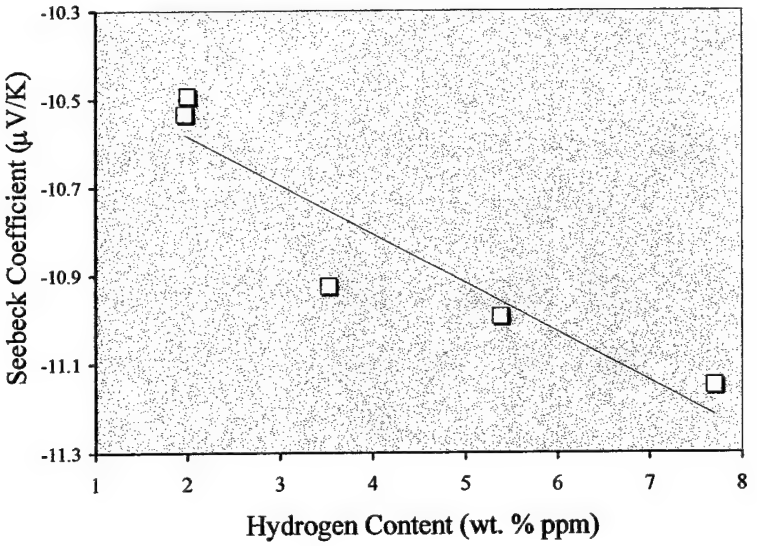

Fig. 32. Correlation of Seebeck Coefficient with hydrogen content of Invar alloy.

5.2.3.3 Accomplishments of Phase III

1. Thermoelectric (Seebeck) coefficient measurements can be used to rapidly determine the diffusible hydrogen contents in high strength steel welds.
2. Thermoelectric (Seebeck) coefficient measurements will allow diffusible hydrogen contents be determine on the actual welded structure and not just on test coupons used to quantify welding materials and practices.

5.3 Design Requirements for a Rapid Weld Hydrogen Analysis

The design requirements for the further development of apparatus for measuring electronic and magnetic properties are the following:

1. The analytical hydrogen content sensor needs to be accurate and calibratable to hydrogen content as low as 0.1 ml per 100 g of metal (0.1 ppm hydrogen).
2. Measurements must be consistent with measurements performed by using International Standard Organization (ISO) analytical procedures for weld metal hydrogen content.
3. The analytical apparatus must be easy to operate and understood by technicians in welding workplace.
4. The data must be easily acquired and stored electronically.

5. The data need to be interfaced directly to analytical software that can mathematically extrapolate short-term results into the final diffusible hydrogen content.

6. The measurements must be able to be made directly on welds in the welded structure, as well as measured on test coupons.

7. The equipment must be sufficiently durable and light weight to be conveniently used in the welding workplace.

5.4 Assessment of the State of Hydrogen Development

Measurements of electronic, optoelectronic and magnetic properties have been correlated directly to the diffusible hydrogen content in alloys. The theoretical connection between the diffusible hydrogen content and the fundamental understanding of the behavior of hydrogen in metals and alloys has been described. These concepts may lead to development of new advanced methods for hydrogen determination. The next step is the further development of durable hardware, establishment of procedures for welding technicians, development of practices for calibration, verification of consistency with results from ISO testing procedures, round robin testing, and personnel training.

6.0 REFERENCES

1. N, Yurioka and H. Suzuki, 1990. Hydrogen assisted cracking in C-Mn and low alloy steel weldments. *International Materials Review* 35 (4): 217 - 249.
2. D.L. Olson, I. Maroef, C. Lensing, R.D. Smith, W.W. Wang, S. Liu, T. Wildeman, and M. Eberhert, 1996. Hydrogen Management in High Strength Steel Weldments. *Proc. the Joint Seminar, Hydrogen Management in Steel Weldments.* eds. J.L. Davidson, and D.L. Olson, pp. 1-20. WTIA.
3. I. Maroef, D.L. Olson, M. Eberhart, G.R. Edwards, and C. Lensing, 2000. Weld Metal Hydrogen Trapping. *Review paper* Submitted to International Metallurgical Review, Colorado School of Mines.
4. N.R. Quick and H.H.Johnson, "Diffusivities of Hydrogen and Deuterium in Iron", 49-506 deg C, *Acta Metall.*, 25, p. 891 (1978).
5. H.G. Nelson and J.E. Stein, *NASA Report TND-7265*, NASA Ames Research Center, Moffet Field, CA (1973).
6. A. McNabb and P.K. Foster, *Trans. TMS-AIME*, 227, p. 618-627 (1963).
7. R.A. Oriano, in Proc. Conf. *'Fundamental Aspects of Stress Corrosion Cracking'*, Houston, TX, Sept. 1967, NACE, p. 32-50 (1967).
8. K. Ono and M. Meshi, "Hydrogen Detrapping From Grain Boundaries and Dislocations in High Purity Iron", Acta Metall, 40, 1357-1364 (1992).
9. J.L. Lee and J.Y. Lee, "A Trapping Theory of Hydrogen in Pure Iron", Phil. Mag., 56A (3), 293-309, (1987).
10. I.S. Maroef and D.L. Olson, " *Fundamental Aspects of Hydrogen Trapping in Steel Weld Metal*", to be published in Proc. of Intl. Conf. on Joining of Advanced and Specialty Materials II, Materials Solutions '99, pp 227-235, Cleveland, Ohio, ASM, Materials Park, OH (2000).
11. J.P.Hirth, "Effects of Hydrogen on the Properties of Iron and Steel", *Metall. Trans.*, 13A, p. 861-890 (1980).
12. A.R. Troiano, "Campbell Memorial Lecture", *Trans. ASM*, 52, p. 151-177 (1960).
13. D.L. Olson, I. Maroef, C. Lensing, D. Smith, T. Wildeman, and M. Eberhart, in *'Hydrogen Management in Steel Weldments'* (ed. J.L. Davidson and D.L. Olson), Melbourne, Australia, DSTO and WTIA, p. 1-19 (1996).
14. G.M. Evans and N. Bailey, *Metallurgy of Basic Weld Metal*, p. 212, Abington Publishing, Cambridge, England, UK (1997).
15. R.D. Smith, D.L. Olson, T. Wildeman, D.K. Benson, G.P. Landis, *"Advanced Methods for Hydrogen Determination in High Strength Steel"* to be published in Proc. of Intl. Conf. on Joining of Advanced and Specialty Materials II, Materials Solutions '99, Nov 1-4, 1999, Cleveland, Ohio (1999)
16. L.I. Mikhoudi, M.B. Movchan, I.S. Mel'nik, and V.D. Poznyakov, *Paton Welding Journal*, 2 (12), p. 895-900 (1990).
17. N.G. Efimenko, *Welding Production*, 26 (7), p. 47-49 (1980).
18. H.E. Kissinger, "Variation of Peak Temperature with Heating Rate in Differential Thermal Analysis", J. Research Natl. Bur. Standards, Vol. 57, No. 4, p. 2712 (1956).

19. G.M. Pressouyre and I.M. Bernstein, "A Quantitative Analysis of Hydrogen Trapping", *Metall. Trans.*, 9A, p.1571-1580 (1978).

20. M. Iino, " Trapping of Hydrogen by Sulfur-Associated Defects in Steel", *Met Trans. A*, 16, 401-409 (1985).

21. C. Wildash, R.C. Cochrane, R. Gee, and D.J. Widgery, 1998. Microstructural Factors Affecting Hydrogen Induced Cold Cracking in High Strength Steel Weld Metal. *Proc. 5th Internal Conference, Trends in Welding Research.*, pp. 745-750. ASM International.

22. H.G. Nelson, 1983. *Hydrogen Embrittlement.* Treatise on Materials Science and Technology, 25, Embrittlement of Engineering Alloys. eds. C.L. Briant, S.K. Banerji, pp. 275-395, Academic Press, Inc.

23. H.K. Yalci and D.V. Edmonds, "Application of the Hydrogen Microprint and the Microautoradiography Techniques to a Duplex Stainless Steel", Material Characterization, vol. 34, no. 2, pp. 97-104, 1995.

24. R.O. Ritchie, M.H.C. Cedeno, V.F. Zackay, E.R. Parker, " Effects of Si Additions and Retained Austenite on Stress Corrosion Cracking in Ultrahigh Strength Steels", Metall. Trans. A, Jan. 1978, 9A, (1), 35-40

25. Y.D. Park, "The Role of Retained Austenite in the Hydrogen Management of High Strength Steel Welds", Ms Thesis, Colorado School of Mines, 1999.

26. Otsubo, Syunsuke and Hideshi 1986. *Thermal Analysis of Hydrogen in Steel.* IIW Doc. II-A-680-861993

27. H. Tsubakino, H. Harada, J. Yin, "Thermal release of hydrogen from high strength steel containing retained austenite", ISIJ International (Japan), vol. 39, no. 3, pp. 298-300, 1999.

28. C. Prioul, C.A.V de A. Rodrigues, M. Gross, P. Azou, "Hydrogen Effusion During the Martensitic Transformation of Fe-Ni-C Alloy at Subzero Temperature", Scripta Met., vol. 18, pp. 601-604, 1984.

29. A.S. Grot and J.E. Spruiell, "Microstructural Stability of Titanium-Modified Type 316 and Type 321 Stainless Steel", Met. Trans. A, vol. 6A, Nov, pp. 2023-2030, 1975.

30. American Welding Society 1993. *Standard Methods for Determination of Diffusible Hydrogen Content*: ANSI/AWS A4.3-93, AWS, Miami, FL.

31. M. A. Quintana, 1984. A Critical Evaluation of the Glycerin Test. *Weld. J.* 63 (5), pp. 141s-149s.

32. D.J. Kotecki and R.A. LaFave, 1985. AWS A5 Committee Studies of Weld Metal Diffusible Hydrogen. *Weld. J.* 64 (3), pp. 31-37.

33. L.C. Abreu, P.J. Modenesi, and P.V. Marques, 1994. A Comparative Study of Techniques to Measure Diffusible Hydrogen Content of Welds. IIW Doc. II-A-908.

34. British Standards Institution 1988. Primary Method for the Determination of Diffusible Hydrogen in Manual Metal Arc Ferritic Steel Weld Metal. BS 6693.

35. M.A. Quintana, and J.R. Dannecker, 1988. Diffusible Hydrogen Testing by Gas Chromatography. *Hydrogen Embrittlement: Prevention and Control.* ASTM STP 962, ASTM, Philadelphia, PA, pp. 247-268.

36. L. J. Radziemski, T.R. Loree, D.A. Cremers, and N.M. Hoffman, 1983. Time Resolved Laser Induced Breakdown Spectroscopy of Aerosols. *Anal. Chem.* 55, pp. 1246-1252.

37. D.A. Cremers and L.J. Radziemski, 1983. Detection of Chlorine and Fluorine in Air by Laser Induced Breakdown Spectroscopy. *Anal. Chem.* 55, pp. 1252-1256.

38. B.K. Zuev, V.P. Velyukhanov, Y.A. Kulakov, L.L. Kunin, and G.V. Mikhailova, 1979. Separate Determination of Surface and Volume Content of Oxygen and Hydrogen in Metal Films. *Zhur. Anal. Khimii* 34 (5), pp. 940-943.

39. V.S. Sevast'yanov and B.K. Zuev, 1990. Determination of Crater Volume in Laser Sampling of Materials. *Zhur. Anal. Khimii* 45 (2), pp. 260-264.

40. V.S. Sevast'yanov, B.K. Zuev, N.E. Babulevich, and N.P. Norikov, 1990. Special Features of Generation of Hydrogen From Kh18N10T Steel in Tensile Loading. *Fiz. Khim. Mek. Mater.* 26 (4), pp. 47-50.

41. V.S. Sevast'yanov, B.K. Zuev, and G.V. Mikhailova, 1990. Determining Hydrogen in Titanium Surfaces by Laser Mass Spectrometry. *Zhur. Anal. Khimii* 45 (11), pp. 2231-2234.

42. B.K. Zuev, L.I. Kordonskii, and I.L. Skryabin, 1990. Local Dissolution of Solid Samples Using a Laser. *Zhur. Anal. Khimii* 46 (7), pp. 1268-1271.

43. V.S. Sevast'yanov, B.K. Zuev, and G.V. Mikhailova, 1991. Determination of Hydrogen in Stressed Materials by Laser Source Mass Spectrometry. *Zhur. Anal. Khimii* 46 (9), pp. 1747-1753.

44. B.K. Zuev and O.K. Timonina, 1996. The Investigation of Hydrogen Redistribution Under a Tensile Load. *Hydrogen Effects in Materials*, TMS, Warrensdale, PA, pp. 97.

45. K. Ito and T, Ohgami, 1992. Hydrogen Detection Based on Coloration of Anodic Tungsten Oxide Film. *Appl. Phys. Lett.* 60 (8), pp 938-940.

46. M. Seibert, T. Flynn, D. Benson, E. Tracy, and M. Ghirardi, 1997. Development of Selection and Screening Procedures for Rapid Identification of H_2 Producing Algal Mutants With Increased O_2 Tolerance. *Proceedings of the 1997 Biohydrogen Meeting,* Waikoloa, HI, pp. 227-234.

47. O. Bernauer, J. Topler, D. Noreus, R. Hempelmann, and D. Richter, *Int. J. Hydrogen Energy*, 14(3), 187-200 (1989).

48. R.D. Smith II, D.K. Benson, D.L. Olson, and T.R. Wildeman, *Proceedings from Photonics West 2000 Conference, SPIE*, Vol. 3945, pp 174-184, (2000).

49. R.D. Smith II, D.K. Benson, D.L. Olson, J.R. Pitts, and B.S. Hoffheins, *Advances in Low Cost Hydrogen Sensor Technology, American Chemical Society Review*, Plenum Publishing Co. (2000).

50. R.D. Smith II, D.K. Benson, I. Maroef, D.L. Olson, and T.R. Wildeman, *Welding J.,* 80(5), 115s-121s (2001).

51. C.D. Gelatt, *Theory of Alloy Phase Formation*, TMS/AIM, Warrendale, Pa, p 451 (1980).

7.0 PUBLICATIONS, THESIS, PATENTS, AND HONORS FROM THIS ARO CONTRACT

7.1 Publications

1. J.L. Davidson and D.L. Olson (Editors), "Hydrogen Management in Steel Weldments", Conf. Proceedings, pp. 1-181, Melbourne, October 23, 1996, ISBN 0-7311-0809-4, WTIA, Brighton, Vic., Australia (1997).
2. D.L. Olson, I. Maroef, and C. Lensing, "The Role of Hydrogen Trapping in Hydrogen Management of Steel Welding", Proc. Indian Welding Seminar (NWS '97), pp. 9-24, Bangalore, India, December 11-13, Indian Institute of Welding, Bangalore Branch, (1997).
3. I. Maroef, D.L. Olson, and G.R. Edwards, "Hydrogen Assisted Cracking in High Strength Steel Weldments", Proc. of International Conference on "Welding and Related Technologies for the XXI Century", Kiev, Ukraine, November (1998), pp. 166-176 (in Russian) and in Welding and Surfacing Review, 1998, vol. 12, pp. 209-225 (in English) (1998).
4. W.J. Engelhard, D.L. Olson, and B. Mishra, "Dissolution of Gaseous Hydrogen in High Strength Steels at Elevated Temperature", Conf. Proc. of Advanced and Specialty Materials, "Dissolution of Gases Hydrogen in High Strength Steels at Elevated Temperatures", pp. 133-140, ASM, Materials Park, OH (1998).
5. K.S. Johnson, S. Liu, and D.L. Olson, "Hydrogen Control and Microstructural Refinement of Structural Steel Welds Using Fluoride-Containing FCAW Electrodes", Prod. 17th Intern. Conf. on Offshore Mechanics and Arctic Engineering, ASME/OMAE, Paper OMAE-98-2801, Lisbon, Portugal, July 6-10 (1998).
6. S. Liu, D.L. Olson, and S. Ibarra, "Critical Issues on Quality Underwater Wet Welding: A Review", Proc. Mexican Welding Conference: Memorias Primer Simposium Internacional de Soldadus (SIS '98), pp. 69-91, Monterray, N.L., Mexico, March 12-14 (1998).
7. W. Wang, S. Liu, and D.L. Olson, "Computer Simulation of Hydrogen Diffusion for Underwater Welding", OMAE Paper 98-2205, ASME, Philadelphia, PA, July 6-9 (1998).
8. M.D. Clark and D.L. Olson, "The Role of Welding Parameters in Hydrogen Management", Proc. of Hydrogen Management of High Strength Steel Welds, pp. 215-228, CANMET, Ottawa, Ontario, Canada (1999).
9. M.E. Eberhart, D.L. Olson, and I. Maroef, "Modeling Hydrogen Behavior", in Hydrogen Management for Welding Applications, pp. 111-122, Publ. Materials Technology Laboratory/CANMET, Ottawa, Canada (1999).
10. Y. Park, A. Landau, G.R. Edwards, and D.L. Olson, "The Role of Retained Austenite in the Hydrogen Management of High Strength Steel Welds", Proc. of Int. Conf. on Trends in Welding Research, pp. 31-36, Pine Mtn., GA, ASM, Materials Park, OH (1999).
11. J.E.M. Braid, C.V. Hyatt, D.L. Olson, and G.N. Vigilante, Hydrogen Management for Welding Applications, pp. 1-282, Proc. Intern. Workshop, October 6-8, 1998, ISBN: 0-662-27989-1, CANMET, Ottawa, Canada (1999).
12. R.D. Smith III, D.K. Benson, G.P. Landis, D.L. Olson, and T.R. Wildeman, "Advanced Methods for Hydrogen Determination in High Strength Steels", in Joining of Advanced and Specialty Materials II, ASM Conf., Cincinnati, OH, November 1-4, 1999, pp. 275-283, ASM, Materials Park, Ohio (2000).

13. I.S. Maroef, Y.D. Park, C. Lensing, A. Landau, and D.L. Olson, "Hydrogen Trapping of High Strength Steel Weld Metal", in Joining of Advanced and Specialty Materials II, pp. 284-291, ASM Conf., Cincinnati, OH, November 1-4, 1999, ASM, Materials Park, OH (2000).

14. I.S. Maroef and D.L. Olson, "Fundamental Aspects of Hydrogen Trapping in Steel Weld Metal", in Joining of Advanced and Specialty Materials II, pp. 227-235, ASM Conf., Cincinnati, OH, November 1-4, 1999, ASM, Materials Park, OH (2000).

15. I.S. Maroef and D.L. Olson, "The Effect of Composition, Hydrogen Traps and Thermal on Hydrogen and Distribution in Steel", Proc. 19th ASM Heat Treating Society Including Steel Heat Treating in the New Millennium, pp. 543-551, November 1-4, 1999, Cincinnati, OH, ASM International, Materials Park, OH (2000).

16. R.D. Smith II, D.L. Olson, T.R. Wildeman, and D.K. Benson, "Fiber Optic Sensor for Diffusible Hydrogen Determination in High Strength Steel", Proc. SPIE Photonics 2000, SPIE Vol. 3945, pp 174-184, January 25, 2000, San Jose, CA (2000).

17. R.D. Smith II, G. Plandis, I. Maroef, D.L. Olson, and T.R. Wildeman, "The Determination of Hydrogen Distribution in High Strength Steel Weldments: Part I: Laser Ablation Methods", submitted to Welding Journal, Vol. 80, pp 115s-121s (2001).

18. R.D. Smith II, B.K. Benson, I. Maroef, D.L. Olson, and T.R. Wildeman, "The Determination of Hydrogen Distribution in High Strength Steel Weldments: Part II: Optoelectronic Diffusible Hydrogen Sensor", Welding Journal, Vol. 80, pp 122s-126s (2001).

19. S. Liu, I. Maroef, D.L. Olson, and M. Matsushita, "Hydrogen Management Strategies in Flux-Related Arc Welding", Proc. of IIW Asian Pacific Intn. Congress, October 29-November 2, 2000, Vol. 1, paper 10, p. 12, Melbourne, Victoria, Australia (2000).

20. Y.D. Park, C. Lensing, I. Maroef, D.L. Olson, and Z. Gavra, "Advances in Hydrogen Management for High Strength Steel", 9th CF/DRDC MEETING on NAVAL APPLICATIONS OF MATERIALS TECHNOLOGY, Dartmouth, Nova Scotia, CANADA, p. 215-231 (2001).

21. Y.D. Park, I.S. Maroef, A. Landau, and D.L. Olson, "Retained Austenite as a Hydrogen Trap in Steel Welds, Welding J. Vol 80, pp (2001).

22. M.E. Eberhart, D.L. Olson, and I. Maroef, "Modeling Hydrogen Behavior", in Hydrogen Management for Welding Applications", pp 111-122, Publ. Materials Technology Laboratory/ CANMET, Ottawa, Canada (1999).

23. M.D. Clark and D.L. Olson, " The Role of Welding Parameters in Hydrogen Management", Proc. Of Hydrogen Management of High Strength Steel Welds, pp 215-225, CANMET, Ottawa, Ontario, Canada (1999).

7.2 Theses

1. Rodney D. Smith II (1999),"Method for the Determination of Hydrogen Distribution in High Strength Steel" (With Professor Thomas R. Wildeman), (Phy. Applied Chemistry).

2. Iman Maroef (1999),"Fundamental Study of Hydrogen Trapping in Steel Weld Metal". (Ph. D. Met. Eng)

3. Yeong-Do Park (1999),"The Role of Retained Austenite in Hydrogen Management in High Strength Steel Weldments" (MSc Met. Eng.)

4. Chad Lensing (2001), "The Utilization Of Yttrium Hydrogen Trap And Welding Parameters In Managing Hydrogen Content In Welding High Strength Low Alloy (HSLA) Steel" (PhD Met. Eng.)

7.3 Patents

R.D. Smith, D.K. Benson, T. R. Wildeman, and D.L. Olson, "Sensor for Testing the Diffusible Hydrogen Content of Welded Steel", U.S. Provisional Patent Application, NREL File No. ProV/99-03, June 7, 1999.

7.4 Honors

1999 TTCP Achievement Award, U.S. Dept. of Defense, Pentagon, Washington, D.C. (April 2000).

8.0 LIST OF PARTICAPATING SCIENTIFIC PERSONNEL

1. Dr. David L. Olson, Principal Investigator
2. Dr. Thomas R. Wildeman (Augmentation Program)
3. Rodney D. Smith II (Received Ph. D. Applied Chemistry, Colorado School of Mines, Golden, CO December 1999) (Augmentation Program)
4. Iman Maroef (Received Ph.D. Met. Eng, Colorado School of Mines, Dec. 1999)
5. Chad Lensing (Received Ph.D. Met. Eng. Colorado School of Mines. Dec. 2000)
6. Yeong-Do Park (Received Msci. Met. Eng., Colorado School of Mines; May, 1999, continues for PhD degree)